

SPECTACULAR POST-PERHELION TAILS OF BRIGHT KREUTZ SUNGRAZERS

ZDENEK SEKANINA

La Canada Flintridge, California, U.S.A; *ZdenSek@gmail.com* 4800 Oak Grove Drive, Pasadena, CA 91109, U.S.A.

Version October 10, 2023

ABSTRACT

A vast majority of bright comets between the late 2nd century and the early 18th century, moving in potentially Kreutz orbits according to Hasegawa & Nakano (2001), was first sighted between 2 and 16 days after perihelion, thanks to the spectacular tails that they were then displaying. In this paper I examine the basic properties of the post-perihelion tails of the three brightest Kreutz sungrazers of the 19th and 20th centuries — the Great March Comet of 1843 (C/1843 D1), the Great September Comet of 1882 (C/1882 R1), and Ikeya-Seki (C/1965 S1). As the pre-perihelion tail of a sungrazer sublimates completely at perihelion, the development of its post-perihelion tail starts from scratch. In the early days after perihelion, the tail length grows rapidly on account of the plasma component. At some point the dust tail takes over, reaching a peak length weeks later. As the geocentric distance continues to increase and the surface brightness to decline, the tail's shortening eventually sets in. The dust tails of Ikeya-Seki and the 1843 sungrazer contained grains subjected to solar radiation pressure accelerations not exceeding 0.6–0.7 the solar gravitational acceleration, the dust tail of the 1882 sungrazer was more complex. For weeks this comet appeared like a comet in a comet, a result of disintegration of a distant companion near perihelion. Evening Kreutz sungrazers are found to have longer tails than morning ones because of geometry. Other issues are discussed and extensive sets of tail data are provided.

Subject headings: comets general: Kreutz sungrazers; comets individual: C/1843 D1, C/1882 R1, C/1965 S1, C/2011 W3; methods: data analysis

1. INTRODUCTION

Inspection of Hasegawa & Nakano's (2001) collection of historical appearances of potential Kreutz sungrazing comets suggests that nearly 90 percent of these objects recorded between the end of the 2nd century and the beginning of the 18th century were first sighted 2–16 days after perihelion, the average being 8.5 days. Because this happens to be the time when a bright sungrazer displays a spectacular tail that is much more conspicuous than the head, the potential Kreutz sungrazers undoubtedly were in the given period of time detected thanks to their post-perihelion tails.

The objective of this paper is to learn about these post-perihelion tails by examining the tails of the brightest Kreutz sungrazers of the past two centuries and presuming that their properties are representative of the historical sungrazers. The primary tasks are the discrimination between the dust and plasma tails and the determination of a peak solar radiation pressure acceleration that grains in the dust tails are subjected to, a measure that governs the tail length.

2. POST-PERHELION TAILS OF SUNGRAZERS IKEYA-SEKI AND LOVEJOY

Very compelling evidence on the nature of the post-perihelion tails of the Kreutz sungrazers results from careful inspection of the observations of comets Ikeya-Seki (C/1965 S1) and Lovejoy (C/2011 W3), the two best studied sungrazers over the past hundred years. However, the tail investigations of the two objects work with greatly different data sets because these comets were not at all alike. Even though the nucleus of Ikeya-Seki split near perihelion into *two sizable* fragments, the comet survived (e.g., Marsden 1967). On the other hand, the nu-

cleus of Lovejoy disintegrated about 40 hours after perihelion (Sekanina & Chodas 2012). As a result, unlike in the case of Ikeya-Seki (and other surviving sungrazers), comet Lovejoy's post-perihelion (or, more precisely, post-collapse) tail was pure dust, as no source of gas was any longer available to replenish its ion tail.

In their investigation of Lovejoy, Sekanina & Chodas (2012) detected considerable sublimation of dust in close proximity of perihelion, at heliocentric distances smaller than 1.8 solar radii, and suggested that the dust particles in the tail were magnesium-rich olivine-based silicates, subjected to radiation pressure accelerations of up to 0.6 the Sun's gravitational acceleration. This limit was also consistent with most of the 54 post-perihelion tail length estimates collected from the period of 2011 December 21 to 2012 March 16, with the inferred ejection times confined to between ~ 7 hours after perihelion and the time of disintegration, some 30+ hours later. Thompson (2015) measured a high degree of polarization in Lovejoy, increasing with distance from the nucleus and reaching as much as 58 percent or more in distant parts of the tail; he independently invoked submicron-sized magnesium-rich silicate grains to explain his findings.

By contrast, numerous photographic and spectral observations of the post-perihelion tail of comet Ikeya-Seki indicated that it was a mixed plasma-sodium-dust feature, with a dominant optical contribution from microscopic dust and with plasma instabilities responsible for superposed multiple helical structures (e.g., Krishan & Sivaraman 1982).

Figure 1 is a nice example showing the dominance of dust in the tail of Ikeya-Seki, while the plasma features are enhanced in the tracings in Figure 2 (Larson 1966). The properties of the dust in the tail of Ikeya-Seki were

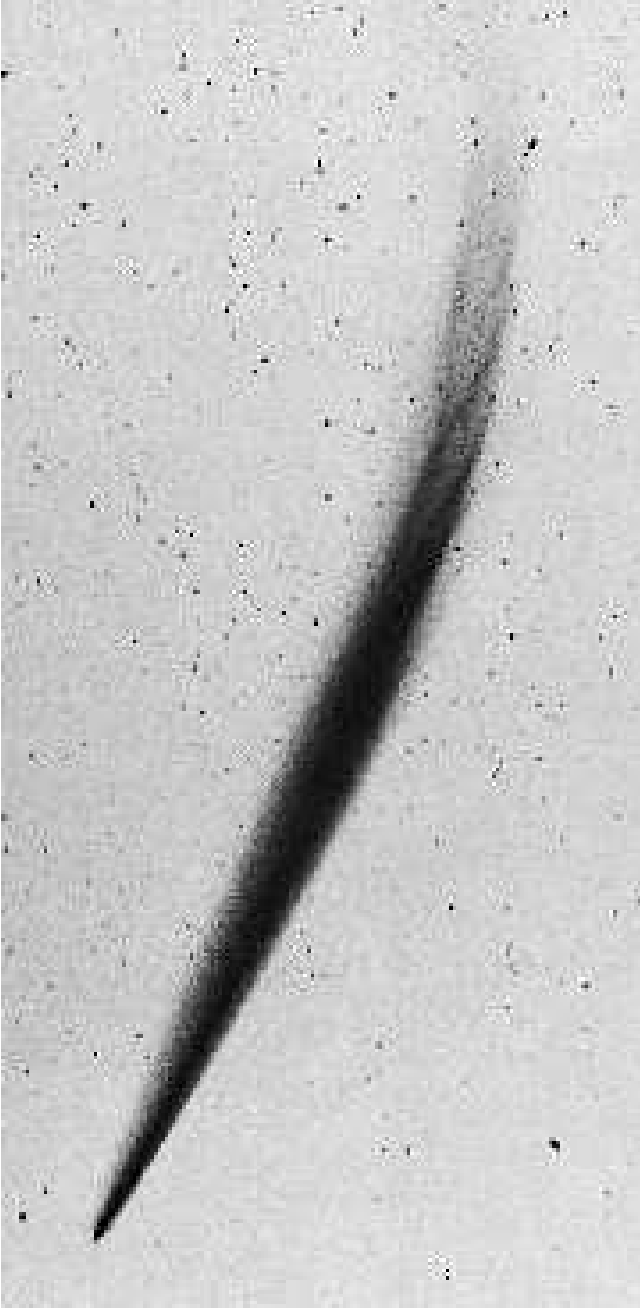


Figure 1. A 45-sec exposure of comet Ikeya-Seki by D. Milon and S. M. Larson, Lunar and Planetary Laboratory, with a 3.5-cm $f/2.8$ camera and Tri-X panchromatic emulsion on 1965 October 30.51 UT. The tail was 21° long. (From Larson 1966.)

examined among others by Matyagin et al. (1968), Weinberg & Beeson (1976a, 1976b), Krishna Swamy (1978), Saito et al. (1981), and Gustafson (1985). Using a variety of methods (polarization, solar radiation pressure effects, microwave analogs), these authors consistently concluded that the brightness of the post-perihelion tail was mostly due to scattering of sunlight by microscopic silicate grains. Matyagin et al. (1968) detected polarization in the dust tail in excess of 70 percent, in fair agreement with Thompson's (2015) measurements in the tail of comet Lovejoy nearly 50 years later.

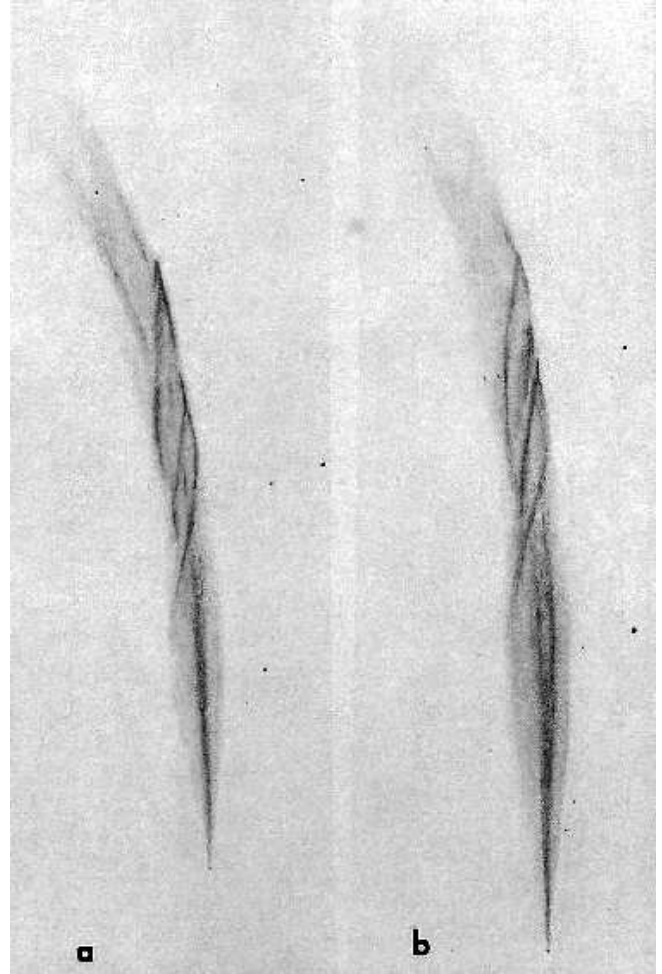


Figure 2. Tracings of the helical structure in the tail of comet Ikeya-Seki, made by S. M. Larson from plates taken with the 18-cm $f/7$ Bailey astrograph of Steward Observatory; (a) October 27.52 UT, tail 15° long; (b) October 28.52 UT, tail 17° long. North is to the left, west is up. (From Larson 1966.)

Milon (1969) published a comprehensive summary of the post-perihelion tail observations of comet Ikeya-Seki made by members of the Association of Lunar and Planetary Observers. The list contained 80 estimates of the tail length obtained between 1965 October 25 and December 4, some of them visual, other measured on photographs. Another dataset by Milon (1969) provided information on the projected orientation of the tail's spine between October 25 and November 6.

Besides Larson's (1966) and Milon's (1969) papers, independent data on the post-perihelion tail of comet Ikeya-Seki were published by Antal (1965), by Tammann (1966), and especially by Bennett & Venter (1966), who included the coordinates of the tail's tip. A large fraction of the visual observations of the length and orientation of the comet's post-perihelion tail is available from six issues of the *International Comet Quarterly* (Green 1982, 1985, 1987, 1991, 1993, 2001). The grand total of observations covers a period of 85 days and it is presented in Appendix A: the tail lengths in Table A-1, the position angles in Table A-2.

2.1. Dust Tails of SOHO and STEREO Dwarf Kreutz Sungrazers

I now briefly digress from the main subject of the paper to say a few words in support of the results presented in the previous section.

Since the dwarf Kreutz sungrazers perish before reaching perihelion, they provide no data directly relevant to the post-perihelion tails of the bright members of the system. However, given that all Kreutz sungrazers are fragments of a single body — are their basic tail properties dependent on the fragment’s size. Two investigations suggested that the dust in brighter, tail-displaying, dwarf sungrazers observed with the coronagraphs on board the SOHO and STEREO space observatories was subjected to solar radiation pressure accelerations not exceeding ~ 0.6 the Sun’s gravitational acceleration, just as the dust in comet Lovejoy. This result was derived by Sekanina (2000) from analysis of the tails of 11 SOHO sungrazers in the years 1996–1998 and independently by Thompson (2009), who triangulated the tail of a bright dwarf comet C/2007 L3, using data from the coronagraphs on board the two STEREO spacecraft.

2.2. Dust in Post-Perihelion Tail of Comet Ikeya-Seki

Even though dust was not the only constituent of the spectacular, early post-perihelion tail of comet Ikeya-Seki, it was the primary component and progressively the more so the farther was the comet from the Sun. Given that dust in the tails of comet Lovejoy and dwarf Kreutz sungrazers is consistently subjected to the same peak radiation pressure acceleration, one should test whether the massive amount of data on Ikeya-Seki’s post-perihelion tail length, collected in Appendix A, is also in line with this result. For an assumed radiation pressure acceleration of 0.6 the solar gravitational acceleration, the *predicted* length and orientation of this comet’s tail are at several post-perihelion times plotted in Figure 3 as a function of the ejection time. To develop a simple model for variations with time in the length of this sungrazer’s tail, it is first necessary to examine the relationship between the dust tail orientation (i.e., position angle) and the ejection time of the dust at the tail’s end point.

A list of the observed orientations of the tail of comet Ikeya-Seki is presented in Table A–2 of Appendix A and the data are plotted in Figure 4. Some of the observations made between 5 and 20 days after perihelion — especially the photographic ones — show that the axis of the tail essentially coincided with the direction of the prolonged radius vector, an effect suggestive of a plasma tail. On the other hand, at the times of more than 20 days after perihelion, most of the plotted points are at the position angles greater than the antisolar direction, implying the presence of a dust tail.

Comparison of Figures 3 and 4 shows that with a possible exception of the earliest post-perihelion observations, the dust ejecta determining the tail length were those leaving the nucleus 5 hours after perihelion or later. The dust tail is predicted to have extended over approximately 10° on October 26, $\sim 18^\circ$ on October 31, $\sim 23^\circ$ on November 5, $\sim 25^\circ$ on November 10, over not more than 27° on November 15, and over less than 27° on November 20 and beyond.

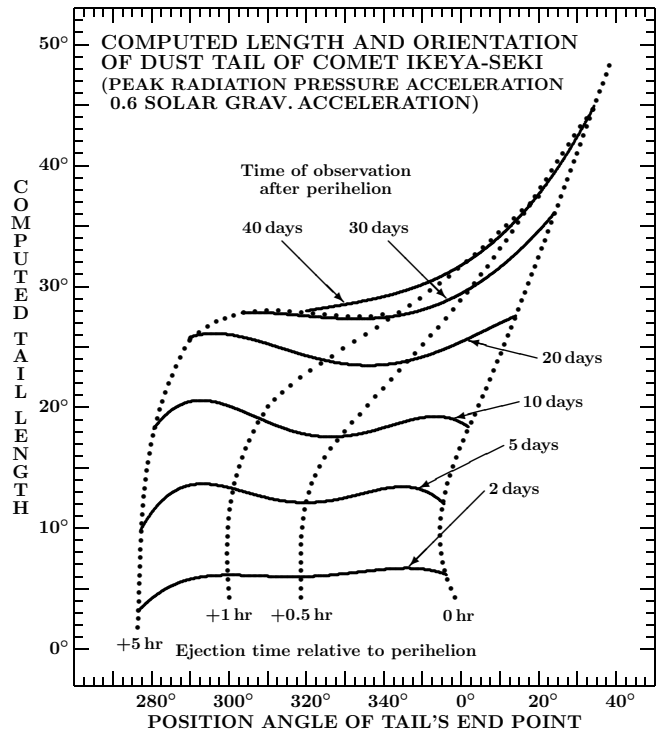


Figure 3. Dust tail length, computed for a peak radiation pressure acceleration of 0.6 the solar gravitational acceleration, against the position angle of the end point. The solid curves apply to six observation times, the dotted curves to four ejection times.

The reported post-perihelion tail lengths of comet Ikeya-Seki, summarized in Table A–1 of Appendix A, are compared with the predicted length of the dust tail in Figure 5. At observation times $t_\pi < t_{\text{obs}} \leq t_\pi + 45$ days (t_π being the perihelion time) the predicted length ℓ was

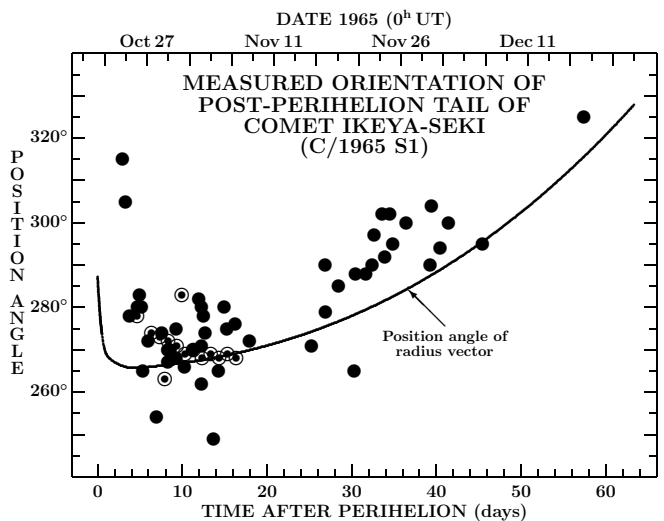


Figure 4. Reported position angles of the post-perihelion tail of comet Ikeya-Seki. The solid circles are visual observations, the circled dots photographic observations. The temporal variations in the position angle of the prolonged radius vector are depicted by the curve. The tail orientation nearly coincided with the antisolar direction in the period of 5–20 days after perihelion. Systematic deviations are apparent at more than 20 days after perihelion.

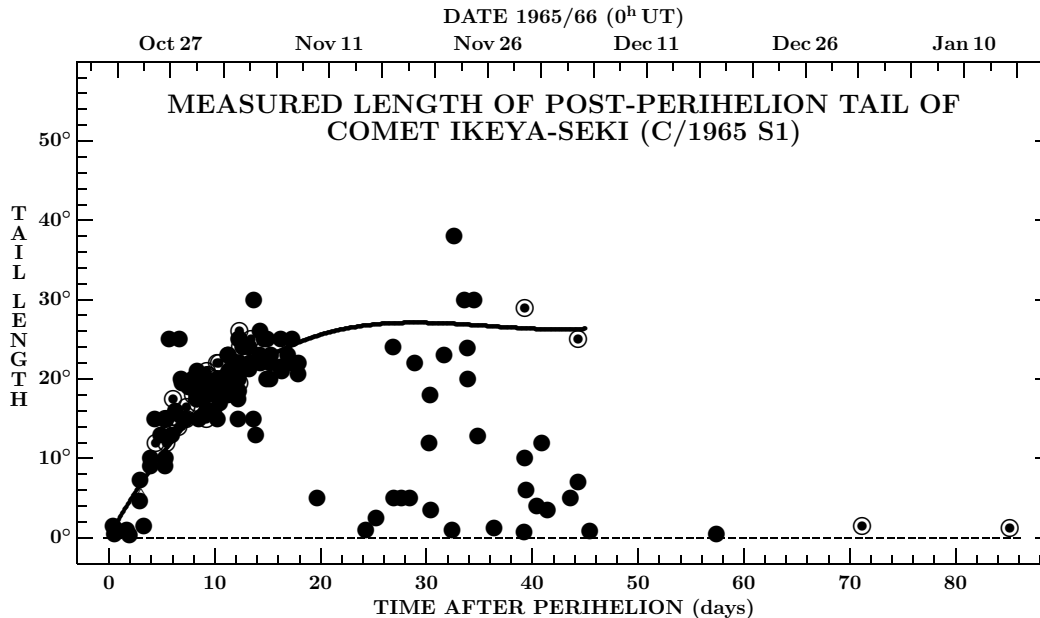


Figure 5. Reported lengths of the post-perihelion tail of comet Ikeya-Seki. The solid circles are visual observations, the circled dots photographic observations. The predicted dependence of the dust tail length on time, described in the text, is depicted by the thick curve.

approximated by a polynomial

$$\ell = 241^\circ \cdot \tau (1 - 2.9\tau + 2.7\tau^2), \quad 0 \leq \tau \leq 0.45, \quad (1)$$

where $\tau = (t_{\text{obs}} - t_\pi)/100$ and $t_{\text{obs}} - t_\pi$ is in days.

The observed and predicted tail lengths are in fair agreement up to about 20 days after perihelion (i.e., November 10). I conclude that the fundamental assumption of a peak radiation pressure acceleration of 0.6 the solar gravitational acceleration once again appears to fit. As the surface brightness of the tail was decreasing with time, nearly all reported tail lengths farther from perihelion determined visually diminished very rapidly, while the predicted lengths compared favorably with the lengths determined photographically until more than 40 days after perihelion (i.e., early December 1965), as seen from Figure 5.

3. POST-PERHELION TAIL OF GREAT SEPTEMBER COMET OF 1882

The post-perihelion tail of the Great September Comet of 1882 (C/1882 R1) was more complex, even though it was not reported to display the helical structures seen early after perihelion in the tail of comet Ikeya-Seki. To determine the type of the 1882 comet’s tail, it was essential to learn its length and orientation in the first days after the comet emerged from the Sun’s rays in late September.

As is apparent from a summary of tail length observations in Table B–1 of Appendix B, the first determination of this kind — obtained visually less than six days after perihelion — was reported by Barnard (1884). Although he did not nominally measure the tail’s position angle, he did remark that the tail — very narrow, only about $1^\circ.5$ wide at most, with the boundaries sharply defined — made at the time an angle of 45° with the horizon. This information allows one to derive the tail’s position angle of 262° , within 1° of the radius vector. The tail was 15°

long at the time, and this requires a radial acceleration of about 10 times the solar gravitational acceleration, far beyond the range of dust-grain accelerations, but typical for the plasma tails. At the same time, Barnard also remarked that the tail was slightly convex to its south side, a feature that is characteristic of a dust tail. An obvious conclusion is that, early after perihelion, the 1882 comet too appeared to exhibit a mixed, dust-plasma tail.

Gill (1882) took six photographs of the comet and its tail with a small camera at the Royal Observatory at Cape between 1882 October 20 and November 15 UT; the exposure times were 30 to 140 minutes. However, the photographs appear to have never been examined and no results were published for decades (Gill 1911).

Visually, the post-perihelion tail was observed rather extensively. Five dedicated studies were undertaken by, respectively, Schmidt (1882, 1883) at Athens; Schwab (1883) at sea (on board the ship *Thebes*); Barnard (1883, 1884) at Nashville, Tenn.; E. Frisby, A. N. Skinner, and W. C. Winlock at the U.S. Naval Observatory (Winlock 1884); and Leavenworth & Jones (1914) at the Leander McCormick Observatory. Observations were also secured by André (1882), Ellery (1882a, 1882b), Galle (1882), Kortazzi (1882), Ledger (1882), Palisa (1882), von Engelhardt (1882, 1883), Backhouse (1883), and Gould (1883). The in-depth report by Leavenworth & Jones includes a number of the tail’s drawings as well as their extensive description.

3.1. Schmidt’s Observations of a Bright Spot α'

Schmidt (1882) remarked that the “true” tail, which in the upper part of Figure 6 occupies the general region AA' , was up to 23° long and terminated in a faint, sharp tip. He further noted that parallel to this tail ran a “nebulous tube” (Nebelrohr) BB' that appeared to emanate from a feature located several degrees from the comet’s head, C , sunward (to the east) of it. This fea-

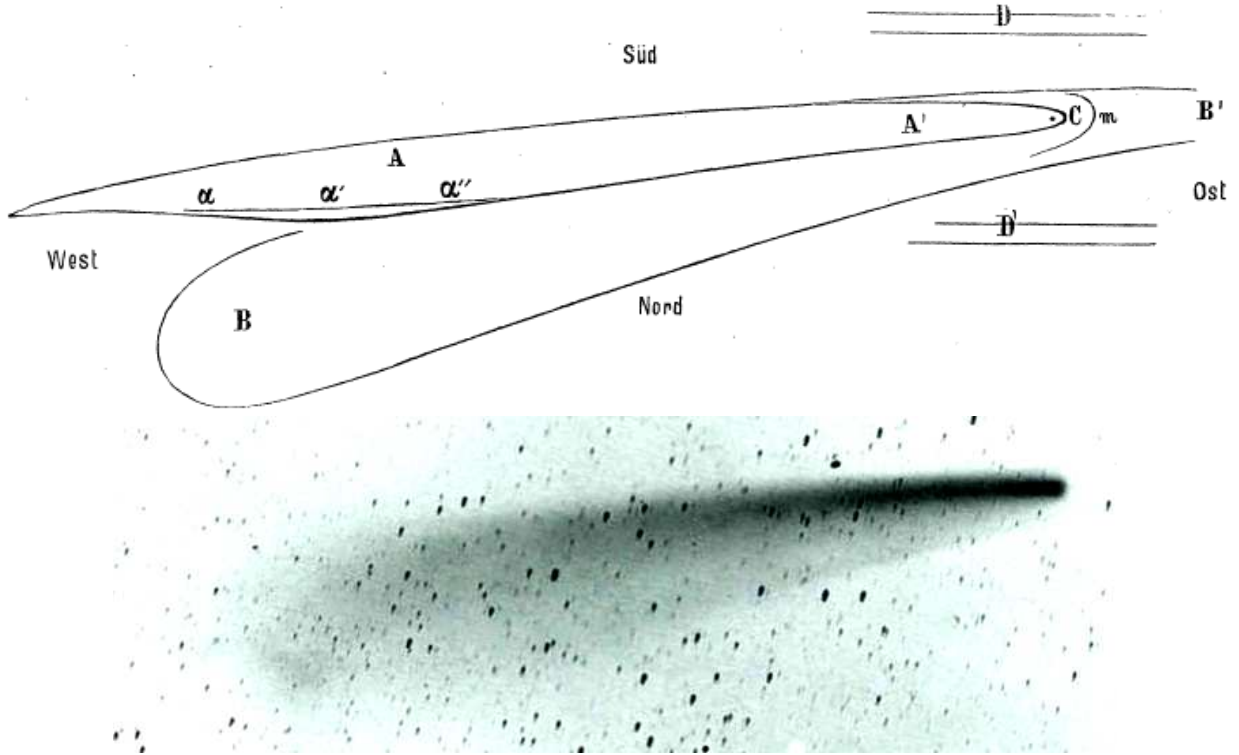


Figure 6. Schmidt’s (1882) schematic drawing of the Great September Comet after perihelion (at the top) and Gill’s (1882) 100-minute exposure of the comet taken with a 6-cm $f/4.4$ camera, attached to the 15-cm Grubb equatorial, on 1882 November 8.06 UT. It is noted that neither the drawing nor the photograph contain any feature that could be classified as belonging to a plasma tail; it is all dust. The photograph has been scaled and rotated to fit approximately the dimensions of the drawing, which refers to a much earlier date and in which the north is down and east to the right. The features of interest to this research are (i) the “true” tail AA' ; (ii) the bright spot α' , which is clearly resolved in the image as an isolated fuzzy cloud 16° to the west-northwest from the head and which in October was at the middle of an elongated feature $\alpha \alpha' \alpha''$; and (iii) the extended region BB' , referred to by Schmidt as a *nebulous tube* (Nebelrohr).

ture was also reported by other observers and extensively described by Schwab (1883); see Section 3.3. In addition to two branches of light, D and D' , and a temporary halo, m , Schmidt also noted, near the northwestern end of the true tail, a strikingly bright “hem” (Saum), $\alpha \alpha' \alpha''$. From November 6 on, the hem’s bright spot α' grew into a distinct, isolated $0^\circ.5$ wide cloud, which is clearly visible in Gill’s 100-minute exposure in Figure 6.

Schmidt provided approximate equatorial coordinates of the feature α' , for the equinox of 1850.0, on 24 occasions between October 6 and November 17 UT, with the times given to 0.1 hr. By converting the coordinates to the equinox of J2000.0 and by computing the topocentric ephemeris for the nucleus at the given times, one can examine the motion of this feature through the tail. The positions as a function of time should provide constraints on both the ejection time and the effective solar radiation pressure that the dust grains making up the feature were subjected to.

The results of the modeled feature are presented in Table 1. Column 2 lists the cometocentric latitude of the Earth, which provides information on the degree of resolution with which we view the motions of features, such as α' , in the orbital plane of the comet. No modeling would effectively be possible, if the angle should be very close to zero, because our view would then be essentially edge-wise. Columns 3 and 4 are the observed polar co-

ordinates of the feature, derived from Schmidt’s original data after they were converted to the equinox of J2000. The last four columns offer the results of the solution that was deemed to provide an optimized approximation, but not a least-squares solution.

Ignoring a potential effect of a separation velocity, the presented fit was obtained for an ejection time, t_{ej} , of 0.9 day after perihelion and an effective radiation pressure acceleration, β_{eff} , of 0.7 the solar gravitational acceleration. The mean residuals were $\pm 0^\circ.82$ in the distance from the nucleus and $\pm 1^\circ.62$ in the position angle. However, even at a radial distance of 17° , slightly exceeding the peak tabulated distance, the mean residual in the position angle would be equivalent to a transverse distance of only $\pm 0^\circ.48$; the uncertainty in the radial distance thus clearly dominated. As seen from Figure 6, the diameter of the feature was about $0^\circ.5$ on November 8, so that the uncertainty exceeded it by a factor of nearly two. Under these circumstances, one should accept the results of modeling with caution.

As Schmidt tried to investigate the feature’s motion himself, he may have noticed how incongruous his measurements were. This may have been the reason for his introduction of four “normal places” by averaging the 24 points. I compare these more representative positions with the same model solution in Table 2. The mean residuals do indeed improve significantly, amounting to

Table 1
Schmidt’s Positional Observations of Feature α' in Tail of Great September Comet of 1882

Time of observation 1882 (UT)	Cometo- centric latitude of Earth	Observation		Model: $t_{ej} - t_{\pi} = +0.9$ day, $\beta_{eff} = 0.7$			
		Distance from head	Position angle	Distance from head	Residual $O - C$	Position angle	Residual $O - C$
Oct 6.15	-11°8	12°7	271°8	9°9	+2°8	271°2	+0°6
8.12	-12.4	11.4	270.9	10.7	+0.7	272.4	-1.5
9.11	-12.8	11.1	271.6	11.1	0.0	273.0	-1.4
10.13	-13.1	10.7	273.6	11.4	-0.7	273.7	-0.1
11.12	-13.4	12.1	273.8	11.8	+0.3	274.4	-0.6
12.14	-13.7	13.0	275.3	12.1	+0.9	275.0	+0.3
13.12	-14.0	13.6	275.1	12.4	+1.2	275.7	-0.6
15.09	-14.6	13.2	280.1	13.0	+0.2	277.0	+3.1
16.10	-14.9	13.9	277.8	13.2	+0.7	277.7	+0.1
17.12	-15.2	13.1	277.0	13.5	-0.4	278.4	-1.4
18.11	-15.5	13.5	277.8	13.7	-0.2	279.1	-1.3
19.11	-15.8	14.3	280.5	14.0	+0.3	279.9	+0.6
23.11	-16.9	14.1	280.3	14.8	-0.7	282.8	-2.5
24.10	-17.2	14.1	281.6	14.9	-0.8	283.6	-2.0
25.14	-17.4	15.2	282.0	15.1	+0.1	284.4	-2.4
Nov 6.10	-20.3	16.0	292.4	16.4	-0.4	294.9	-2.5
7.13	-20.6	15.9	294.5	16.5	-0.6	295.9	-1.4
8.09	-20.8	16.1	295.0	16.5	-0.4	296.9	-1.9
9.10	-21.0	15.9	296.1	16.6	-0.7	297.9	-1.8
10.17	-21.2	16.0	297.8	16.6	-0.6	299.0	-1.2
11.05	-21.3	15.8	299.1	16.6	-0.8	300.0	-0.9
12.08	-21.5	16.4	299.7	16.6	-0.2	301.1	-1.4
15.08	-22.0	16.5	302.2	16.7	-0.2	304.6	-2.4
17.13	-22.3	16.2	307.3	16.7	-0.5	307.2	+0.1

Table 2
Schmidt’s “Normal Places” of Feature α' in Tail of Great September Comet of 1882

Time of observation 1882 (UT)	Observation		Model: $t_{ej} - t_{\pi} = +0.9$ day, $\beta_{eff} = 0.7$			
	Distance from head	Position angle	Distance from head	Residual $O - C$	Position angle	Residual $O - C$
Oct 10.184	11°6	273°6	11°4	+0°2	273°7	-0°1
16.184	13.5	278.2	13.2	+0.3	277.7	+0.5
21.184	14.1	280.5	14.4	-0.3	281.2	-0.7
Nov 10.184	16.0	298.0	16.6	-0.6	297.9	+0.1

$\pm 0^{\circ}.44$ in the distance from the nucleus and $\pm 0^{\circ}.50$ in the position angle, equivalent to $\pm 0^{\circ}.12$ in the angular distance in the transverse direction.

The obvious difference between the dust grains populating the most distant parts of Ikeya-Seki’s tail and the dust that made up the feature α' in the tail of the 1882 comet is in that the latter was ejected from the nucleus later after perihelion than the former. The difference in the effective radiation pressure acceleration appears to be minor. In the context of these inconclusive results it is desirable to examine the tail length and orientation of the 1882 comet.

3.2. Tail Length and Orientation of the 1882 Sungrazer

It is unfortunate that information on the tail orientation of the Great September Comet of 1882 is extremely limited; the set of simultaneous data on the tail’s orientation and length is downright pitiful, ruling out application of the approach employed for Ikeya-Seki. Instead I

used the pairs of the tail length and position angle to determine the corresponding pairs of the ejection time and radiation pressure acceleration, as shown in Table 3.

Table 3
Reports on Orientation of Post-Perihelion Tail of Great September Comet of 1882

Time of observation 1882 (UT)	Observation		Best fit		Observer or source of tail data
	Dis- tance	Pos. angle	$t_{ej} - t_{\pi}$ (days)	β_{peak} (s.g.a.)	
Oct 19.12	276°6	Kortazzi
25.44	13°55	281.4	+1.7	0.8	Jones
31.19	280.5	Kortazzi
Nov 3.45	(5.49)	284.0	Leavenworth
8.06	17	290	+3.1	1.5	Gill’s plate
8.07	17	288.6	+4.3	1.9	Kortazzi
9.41	17.06	291.7	+2.8	1.4	Jones

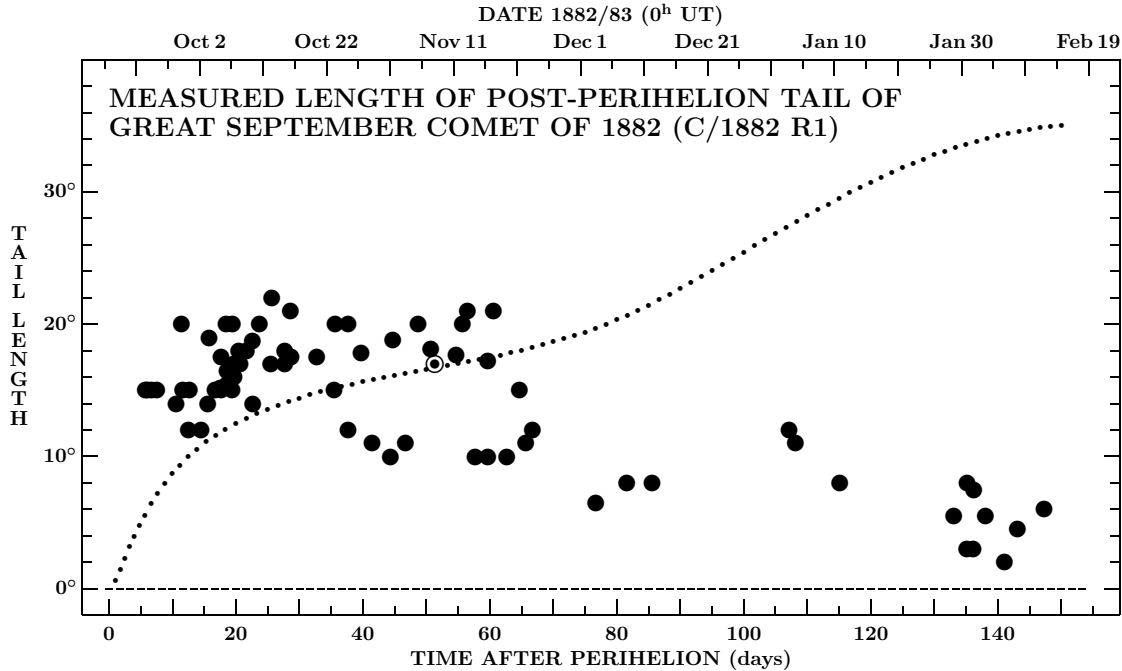


Figure 7. Reported lengths of the post-perihelion tail of the Great September Comet of 1882 from visual observations (solid circles). The circled dot is the single data point based on my estimate of the tail length from Gill’s photograph in Figure 6. The dotted curve shows the dust tail lengths that satisfy the ejection conditions employed for comet Ikeya-Seki in Figure 5.

The position angles listed in the table came from three sources: the observations by Kortazzi (1882) at Nikolayev and by Leavenworth & Jones (1915) at the Leander McCormick Observatory in Virginia were supplemented by my estimate from Gill’s plate in Figure 6. Only four of the seven entries were suitable for analysis, as the other three did not include the tail length or its realistic estimate. Yet, the few numbers suffice to demonstrate significant differences between the 1882 comet and Ikeya-Seki. The particulates defining the length of the 1882 comet’s tail were released from the nucleus at times that lagged the perihelion passage a few days rather than a small fraction of a day and were subjected to much higher radiation pressure accelerations. If correct, this result and an apparent correlation between both parameters in Table 3, imply that unless the reported tail lengths referred to a plasma tail — which is highly unlikely — the dust in the 1882 comet included absorbing grains, contrary to Ikeya-Seki, which contained only dielectric particles.

Similar conclusions are reached from the plot of the 1882 comet’s tail length against the observation time in Figure 7. Although straightforward comparison with Figure 5 indicates that the observed length of Ikeya-Seki’s tail was in fact longer than that of the 1882 sungrazer, the difference was entirely an effect of projection. Figure 7 demonstrates that in the first 30 days after perihelion the tail of the 1882 comet was systematically longer than it should have been, if under the ejection conditions equivalent to those for comet Ikeya-Seki. Interestingly, the tail length estimated from Gill’s photograph in Figure 4 fits the Ikeya-Seki curve just about perfectly. The problem is a difference of tens of degrees in the position angle. And even though, in general, Table 3 and Figure 7 allow either interpretation, Gill’s photograph shows no trace of a plasma tail.

In any case, an obvious question is why are the tails of the two sungrazers — undoubtedly fragments of a common parent — so different? It is conceivable that the culprit was the extensive, multiple fragmentation of the nucleus of the 1882 comet at perihelion. Although Ikeya-Seki split as well, only two persisting components were observed after perihelion. By contrast, the Great September Comet broke up into as many as six major active fragments and the comet’s post-perihelion light curve is known to have been significantly less steep than Ikeya-Seki’s, $r^{-3.3}$ vs $r^{-3.9}$ (Sekanina 2002). The comprehensive fragmentation was likely to bring to the surface the material that otherwise would have stayed hidden in the interior, and the flatter light curve suggests a more substantial contribution to the comet’s activity from the ejecta released farther from perihelion.

3.3. A Comet in a Comet

The feature that Schmidt called the nebulous tube is particularly intriguing. This term is not very fitting and even though Schwab’s is better, the impression that I am getting when looking at their drawings is that of a *comet inside another comet*. The inner comet is the Great September Sungrazer itself, which I will in this section refer to as the *main comet*. The other, with no nuclear condensation and no sunward boundary, I will call the *outer comet*. I am unaware of any other cometary object ever reported to possess such an unusual appearance.

The outer comet must have had a nuclear condensation and sunward boundary at some point in the past. Their loss is a key piece of evidence for the scenario proposed below. I begin with the angular distance between the nucleus of the main comet and the site of the missing nucleus of the outer comet, which is assumed to be closely approximated by the separation of the observed

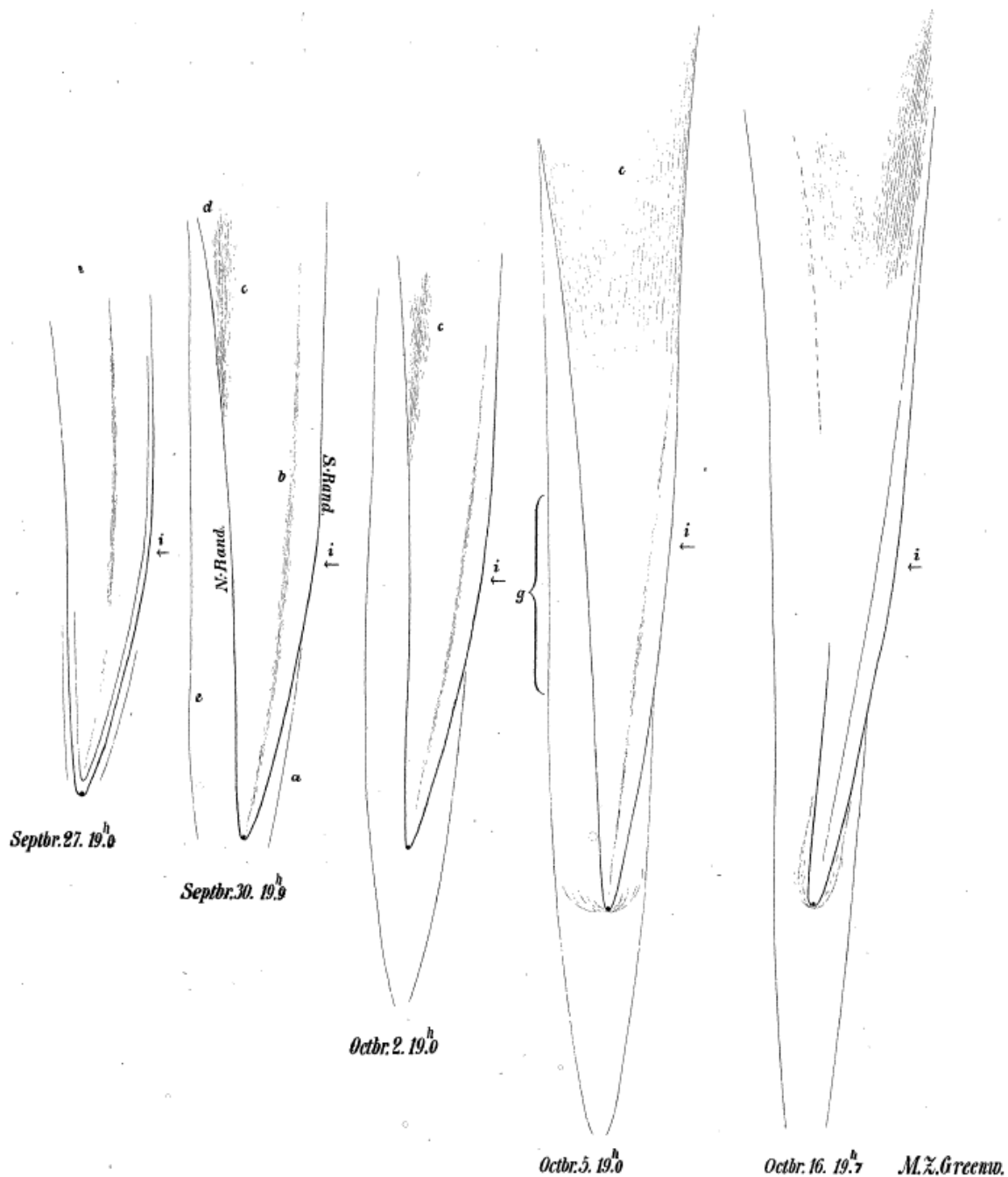


Figure 8. Drawings of the Great September Comet of 1882 by Schwab (1883), who referred to Schmidt's nebulous tube as *Hülle*, i.e., *sheath* or *envelope*. Note that the features make an impression of a comet in a comet. Schwab warned that his drawings were not to the same scale and pointed out that on October 17 the sheath extended over 5° – 6° sunward of the comet's head in an opera glass.

sunward end of the outer comet from the nucleus of the main comet. On Schmidt's drawing in Figure 6 this separation is marked as a distance $B'C$, for which both observers offered their estimates. The important difference was that Schmidt (1882) provided only a general comment, saying that the $B'C$ part of the nebulous tube, seen until November 21, was 1° wide and 3° – 5° long in a seeker telescope; and that it was only 1° – 2° long to the naked eye when the moonlight did not interfere. Schwab (1883), on the other hand, estimated the separation at 5° – 6° in an opera glass and 3° – 4° with the naked eye on

October 17.3 UT. This is important because calculations show that the separation $B'C$ was a strong function of time. Following Schwab, I adopted that the separation between the nuclei equaled $5^{\circ}.5$ on October 17.3 UT.

Next I assumed that the outer comet followed the main comet in the latter's orbit about the Sun, and from the ephemeris I computed the difference in the perihelion time needed to change the orbital position by $5^{\circ}.5$ along the projected orbit on October 17: the result was that the outer comet must have passed the perihelion point 6.76 days *after* the main comet.

Table 4
 Nongravitational Acceleration of the Outer Comet As Function of Location of
 Fragmentation Event in Orbit of Great September Comet of 1882 Needed
 for Main-to-Outer Perihelion Time Difference of 6.76 Days

Fragmentation event ^a			Accel- eration γ (units ^b)	Fragmentation event ^a			Accel- eration γ (units ^b)	Fragmentation event ^a			Accel- eration γ (units ^b)
t_{frg} (yr)	$t_{\text{frg}} - t_{\pi}$ (yr)	r_{frg} (AU)		t_{frg} (yr)	$t_{\text{frg}} - t_{\pi}$ (yr)	r_{frg} (AU)		t_{frg} (yr)	$t_{\text{frg}} - t_{\pi}$ (yr)	r_{frg} (AU)	
1190	51.4	70	1.0	1435	296.4	160	6.6	1648	509.4	150	22.0
1235	96.4	100	1.7	1469	331.1	163	8.0	1688	549.4	140	29.0
1276	137.7	120	2.5	1510	372.0	aph.	10.0	1745	606.4	120	46.3
1333	194.7	140	3.7	1551	413.0	163	12.4	1786	647.7	100	72.4
1373	234.7	150	4.7	1586	447.7	160	15.1	1831	692.8	70	151.0

Notes.

^a t_{frg} is year of the fragmentation event (i.e., time of the outer comet’s birth), t_{π} is the adopted perihelion time of the parent, 1138 Aug 1, and r_{frg} is heliocentric distance of the parent at fragmentation.

^b Units of 10^{-5} the solar gravitational acceleration.

It was now time to propose a scenario for the outer comet, which involved the parent of the 1882 sungrazer — the Chinese comet of 1138 (Sekanina & Kracht 2022) — but was very different from the scenario for comet Ikeya-Seki (Marsden 1967), as one should expect. On the other hand, since the outer comet passed the 1882 perihelion nearly a week after the main comet, the separation must have taken place *very long* before that perihelion (see Sekanina 1982). To survive, the fragment ought to have been fairly massive (although much less massive than the nucleus of the main comet) and subject to a relatively low sublimation-driven nongravitational acceleration, of $\lesssim 10$ units of 10^{-5} the solar gravitational acceleration (in the following: “units”). A fragment of that kind — here the outer comet — orbits the Sun in a gravity field slightly weaker than is the Sun’s gravitational field and, accordingly, its motion is marginally slower than the motion of the principal fragment — here the main comet — hence, the *lag*. The rate of this slowdown in terms of an orbital-period effect, ΔP , can in the *absence of any momentum exchange at breakup* be estimated from a simple equation:

$$\Delta P = \frac{1}{2} 10^{-5} \gamma P, \quad (2)$$

where γ is the nongravitational acceleration (in units) and P is the orbital period of the parent comet (P and ΔP in the same units). Adopting for the outer comet $\gamma \lesssim 10$ units and for the parent sungrazer $P = 744$ yr (1882 minus 1138), one obtains $\Delta P \lesssim 14$ days. More specific conditions are found from the dependence of the nongravitational acceleration γ that implies an 1882 perihelion time difference of 6.76 days as a function of the fragmentation time. These results are presented in Table 4. It follows that the breakup took place most probably on the way to aphelion, not later than in the early 16th century. Otherwise the implied nongravitational acceleration suggests that the outer comet would have been too small to survive intact to the 1882 perihelion.

If the outer comet was involved in any momentum exchange at the time of separation, the numbers in Table 4 should be replaced by another infinite number of possibilities that satisfy the condition of the outer comet lagging 6.76 days behind the main comet at the 1882 perihelion.

In one such scenario, with potentially important implications, the outer comet could have separated from the parent at aphelion in 1510 with a velocity whose transverse component was 3 m s^{-1} in the direction opposite the orbital motion and radial component 0.1 m s^{-1} in the antisolar direction, and then be subjected to a nongravitational acceleration of 5.7 units. Besides arriving at the 1882 perihelion 6.76 days after the main comet, the outer comet would do so in an orbit whose perihelion distance dropped from $1.67 R_{\odot}$ (at a zero separation velocity) to $1.25 R_{\odot}$.

Another set of conditions that the outer comet is expected to satisfy concerns its physical behavior around the 1882 perihelion. The object was either overlooked or too faint to detect before perihelion. Very shortly after perihelion, within several hours or so, the entire body suddenly exploded or collapsed, its mass disintegrating into dust of a wide particle size distribution. The nucleus with its condensation disappeared and much of the dust cloud on the sunward side completely sublimated — especially if the perihelion distance dropped as suggested above — so that in a moment the object gained the appearance consistent with the observations. The dust cloud on the antisunward side survived and instantly began to form the tail. This proposed development is no fairy tale, because at least two sungrazers are known to have disintegrated instantaneously near perihelion. One was comet Lovejoy (C/2011 W3), which suddenly collapsed about 40 hours after perihelion, completely changing its appearance from day to next day (Sekanina & Chodas 2012); the other, apparently smaller object, was the Great Southern Comet of 1887 (C/1887 B1), which is believed to have instantly perished ~ 6 hours after perihelion (Sekanina 1984). Sizewise the outer comet perhaps was in between the two, as it was observed for a little longer than two months following the apparent time of disintegration (see below). Lovejoy was visible for three months and the 1887 sungrazer for barely three weeks.:

Next I examine the timeline of the outer comet. In the adopted scenario the object’s perihelion passage occurred on October 24.5 UT and it disintegrated several hours later, as will be apparent from the following. A reported tail observation of the outer comet on or before this date would invalidate the hypothesis. Schmidt (1882)

observed this feature from October 4 to November 21. Although Schwab (1883) commented on two envelopes on September 24 and 27 (i.e., 25.3 and 28.3 UT), his drawings from five mornings between September 28.3 UT and October 17.3 UT (shown in Figure 8) tell a different story. In the first picture, from September 28.3, the main comet is seen to display *three* envelopes, very close to each other, around *its* nucleus, located at the tip of the condensation; there is no trace of any feature sunward of it. Only the second drawing, from October 1.3 UT, shows an outer envelope, much wider than the main envelope and with the axis shifted slightly to the left (towards the north). The three remaining sketches copy the layout of the second picture, including the asymmetry. However, the sunward extension of the outer envelope is drawn nearly to the tip, especially on the drawings from October 3.3 and 6.3, on which nothing stands in the way to the reader’s overwhelming perception of these features as *a comet in a comet*. Schwab (1883) indicated that he observed the outer comet from October 1.3 to November 13.2 UT (on this last date from Punta Arenas, Chile), when he reported that the object’s figure was still looking like on October 17. The periods of time over which Schmidt and Schwab observed the outer comet were then fairly comparable.

Examining the observed separation between the main comet’s nuclear condensation and the computed position of the outer comet’s disintegrated nucleus was high priority. This distance varied from 11° on September 28.3 to Schwab’s averaged $5^\circ.5$ on October 17.3 UT, so that the outer comet was gradually catching up with the main comet. Interestingly, both Schmidt’s and Schwab’s drawings show the tails of the main and outer comets extending to just about equal distances from the Sun in projection onto the sky, a trait also plainly visible in Gill’s November 8 photograph in Figure 6. Given that the location of the outer comet’s disintegrated nucleus was degrees sunward of the main comet’s nuclear condensation, the deficit had to be made up by the outer comet’s longer projected tail. At first sight, this looks like a difficult condition to satisfy.

To examine this problem in detail, I use the distance of the feature α' from the nucleus of the main comet as a measure of this comet’s tail length, as α' indeed was located near the tail’s very end (Figure 6). This definition of the tail length is convenient, because the position of α' relative to the nucleus is tightly determined by the dynamical parameters (see Tables 1 and 2). Now, let at time t the position vector of the tail’s end point relative to the nucleus be $\mathbf{L}_I(t)$. If the position vector of the nucleus relative to the Sun at time t is $\mathbf{E}_I(t)$, the position vector of the tail’s end point relative to the Sun equals $\mathbf{E}_I^*(t) = \mathbf{E}_I(t) + \mathbf{L}_I(t)$. The position vector $\mathbf{E}_I(t)$ projects onto the plane of the sky as a solar elongation of the main comet’s nucleus, $E_I(t)$, while the position vector $\mathbf{E}_I^*(t)$ as a solar elongation of the tail’s end point, $E_I^*(t)$.

Let, similarly, the position vector of the disintegrated nucleus of the outer comet relative to the Sun at time t be $\mathbf{E}_{II}(t)$. Since the peak solar radiation pressure on dust particles in the tail of the 1882 sungrazer was near $\beta_{\text{peak}} \simeq 2$ units of the solar gravitational acceleration (Table 3), I assume that this too was the peak radiation pressure acceleration that dust particles released from

Table 5
Solar Elongations and Lengths of Main and Outer Comets’ Tails

Date 1882 (UT)	Main comet			Outer comet			ΔE^*	$\Delta\eta$
	E_I	L_I	E_I^*	E_{II}	L_{II}	E_{II}^*		
Oct 1.3	27 $^\circ$.2	7 $^\circ$.6	34 $^\circ$.8	18 $^\circ$.1	11 $^\circ$.7	29 $^\circ$.7	-5 $^\circ$.1	+1 $^\circ$
17.3	46.9	13.5	60.2	41.4	19.7	60.5	+0.3	+3
Nov 4.3	67.7	16.3	83.5	63.7	20.8	82.8	-0.7	+5
21.3	87.7	16.6	103.2	84.6	21.1	101.0	-2.2	+5

Note.

E_I , L_I , and E_I^* are, respectively, solar elongation of the nucleus, projected tail length, and solar elongation of the tail’s end point for the main comet; E_{II} , L_{II} , and E_{II}^* are, respectively, solar elongation of the site of disintegrated nucleus, projected tail length, and solar elongation of the tail’s end point for the outer comet; ΔE^* is the difference between solar elongations of the tail’s end points of the outer and main comets; and $\Delta\eta$ is difference between orientations of the tail’s end points of the outer and main comets; the positive sign indicates that the outer comet’s tail is to the north of the main comet’s tail. The end point of the main comet’s tail is determined by Schmidt’s feature α' , the end point of the outer comet’s tail is determined by motions of dust particles released 0.4 day after perihelion and subjected to radiation pressure acceleration twice solar gravitational acceleration. Outer comet passed perihelion 6.76 days after main comet.

the outer comet were subjected to. And since the ejection of all dust occurred at once, the motion of the particles with β_{peak} determined the tail length of the outer comet. If the position vector of the tail’s end point relative to the location of the disintegrated nucleus at time t is $\mathbf{L}_{II}(t)$, its position vector relative to the Sun equals $\mathbf{E}_{II}^*(t) = \mathbf{E}_{II}(t) + \mathbf{L}_{II}(t)$. The lengths of the position vectors $\mathbf{E}_{II}(t)$ and $\mathbf{E}_{II}^*(t)$ project onto the plane of the sky as solar elongations of, respectively, the outer comet’s disintegrated nucleus, $E_{II}(t)$, and its tail’s end point, $E_{II}^*(t)$.

The choice of the time of the outer comet’s disintegration determines the shift between the tails of the main and outer comets: the earlier the time the farther to the north would the outer comet’s tail be moved and the greater would be the angle subtended by the two tails’ axes. In space this angle, $\Delta\epsilon$, is measured by the scalar product of the two normalized vectors,

$$\Delta\epsilon(t) = \arccos \left[\frac{\mathbf{E}_I^*(t) \cdot \mathbf{E}_{II}^*(t)}{|\mathbf{E}_I^*(t)| \cdot |\mathbf{E}_{II}^*(t)|} \right], \quad (3)$$

and in projection it shows up as a position angle difference $\Delta\eta$; it is positive when the outer comet’s tail is to the north of the main comet’s tail and vice versa. The observations (Figures 6 and 8) consistently show that $\Delta\eta$ was positive but very small, at most several degrees.

Experimentation with the syndynome approach suggested that to fit these conditions on $\Delta\eta$, the disintegration of the nucleus of the outer comet ought to have taken place about 0.4 day after its perihelion passage, i.e., on September 24.9 UT. A solution is presented in Table 5, which shows that, except in early October, the solar elongations of the two tails’ end points, given by ΔE^* , indeed came out to be about equal. The tails’ angular lengths are listed in the table as L_I and L_{II} . Note that because of the projection effects $E_x + L_x \geq E_x^*$ (for $x = I, II$).

This exercise demonstrates that the hypothesis of *a comet in a comet* is plausible, as it is fully supported by the relevant computations.

As the last point I comment on an estimated width of the outer comet's tail and the ramifications for the particle ejection velocities. Schmidt (1882) indicated that the tail was about 1° wide, but provided no details. An assumption that the ejection velocity alone accounts for the tail's width leads to a crude upper limit of $1\text{--}2\text{ km s}^{-1}$. More realistic estimates are a factor of several lower, because the broad range of radiation pressure accelerations contributes significantly to the tail's width as well. Accordingly, the vague data on the velocity of ejecta are not critical and should introduce no major obstacles for accepting the proposed hypothesis.

4. POST-PERHELION TAIL OF GREAT MARCH COMET OF 1843

This sungrazer is believed to have displayed one of the longest and most impressive tails that have ever been observed. I was able to secure a surprisingly large number of estimates of this tail's length by inspecting the major journals of the time. Data were contributed by Cooper (1843), J. G. Galle (Schumacher 1843), Haile (1843), Kay (1843), Knorre (1843), von Littrow (1843), Tucker (1843), Brand (1844), Maclean (1844), E. Dunkin and J. Glaisher (Airy 1845), and Caldecott (1846).

4.1. Observations by C. Piazz Smyth at Cape

A dilligent observer of the comet and major contributor to the pool of available data was C. Piazz Smyth, the first assistant to Director of the Royal Observatory, Cape of Good Hope. When the comet suddenly appeared in close proximity of the Sun at the end of February and in early March, he was, at the age of 24, the only astronomer at the Observatory (Warner 1980). While complaining about the inadequate instrumentation, he managed to secure extensive data on the comet, including numerous drawings of its changing appearance during March. He must have been working extensively on assembling the results — including 11 drawings made between March 3 and 31, five naked-eye views and six telescopic — because he sent them in a letter to the *Monthly Notices of the Royal Astronomical Society* nearly three years after the observations were made (Piazz Smyth 1846). Unfortunately, only a short extract of the accompanying letter was published by the journal's editors and no pictures (judging from the ADS scans).

It was Warner's (1980) publication of detailed extracts from Piazz Smyth's diary that furnished the most welcome data on the tail of the Great March Comet. Included were, in particular, the equatorial coordinates of the end of the tail on nine days between 1843 March 3 and 22, which I combined with a single estimate of the length and orientation by Knorre (1843) on March 17 to examine the comet's tail, using the technique applied to Schmidt's observations of the Great September Comet of 1882. Thanks to these data, I did not have to employ J. F. W. Herschel's reports on stars passing through the tail (e.g., Schumacher 1843; Kapoor 2021), from which the tail orientation should at best be determined only very approximately.

Piazz Smyth was also the author of two paintings whose details are copied below. The first one, made from Table Bay, just to the north of Cape Town, is in Figure 9, showing a daytime sighting of the comet in close proximity of the Sun. From the distance, the comet appears



Figure 9. Daytime sighting of the Great March Comet of 1843 over Table Bay near Cape Town on 1843 Feb. 28.20 UT, less than 30 minutes after sunrise and ~ 7 hours after perihelion. The tail is 1° long. Detail of a painting by C. Piazz Smyth, Royal Observatory, Cape of Good Hope. (National Maritime Museum, London.)

to have been drawn on February 28.20 UT, when it was $1^\circ.1$ from the Sun in position angle of 130° . The comet then moved at a rate of $15'$ per hour. The straight, narrow tail, probably dominated by plasma, was 1° long, pointing in position angle of 134° .

The other of the two paintings, whose detail is reproduced in Figure 10, was made from the area of the Signal Station, Lion’s Rump, to the west of the Royal Observatory, or from a nearby beach. The painting shows the comet shortly before its head set on March 4;¹ the comet was about 17° from the Sun. The very bright star above the comet’s head was β Ceti, while the four stars to the right of the tail were, counterclockwise from the bottom up, η , θ , ζ , and τ Ceti. From an average scale, derived from the distances among these stars, the tail length came out to be 34° long, its position angle 106° , essentially equaling the direction of the prolonged radius vector. Unquestionably, this was a plasma tail, a conclusion implied by both its morphology, length, and orientation. It is noted that, incredibly, the tail was bright enough to reflect in water.

Next, I turned to the available observations of the 1843 comet’s tail orientation and length to determine, as I did for the 1882 comet, the peak radiation pressure acceleration β_{peak} on dust particles located at the tail’s end point and the effective time t_{ej} at which they were ejected. The results of this modeling are presented in Table 6 for ten dates between March 8 and March 22, on which either the coordinates of the tail’s end point or the tail length and orientation (position angle) were measured. Nine of the ten data points were provided by Piazz Smyth (Warner 1980), one came from Knorre (1843). The residuals from two different models fitting the observations about equally well are listed in the table, suggesting that in terms of both the peak radiation acceleration ($\beta_{\text{peak}} \simeq 0.6\text{--}0.7$ the solar gravitational acceleration) and the effective ejection time ($t_{\text{ej}} \simeq 0.2\text{--}0.3$ day after perihelion) the 1843 sungrazer’s behavior resembled that of comet Ikeya-Seki, but differed from the 1882 sungrazer’s.

In column 2 of Table 6 I present — as in Table 1 for the 1882 comet — a cometocentric latitude of the Earth, which determines the foreshortening involved in the observer’s view of the distribution of dust particles in the comet’s orbital plane. The tabulated numbers demonstrate that the geometry of the 1843 encounter of the Earth with the Great March Comet was rather unfavorable, as the latitude was in absolute value smaller than 10° on March 8 and was getting smaller with time. At the time of observation on March 22 the Earth was crossing the plane of the comet’s orbit, so that the observer was looking at the dust tail edge on. At that time the position angle of the observed tail equaled the position angle of the projected orbital plane and provided no information whatsoever on the distribution of dust in the plane, the residuals merely reflecting the errors of observation. The unfavorable geometry was in part to blame for a very little difference in the quality of fit offered by the two tabulated models A and B.

4.2. Tail Length of the 1843 Sungrazer

The tail lengths reported in accessible publications are summarized in Table C–1 of Appendix C and plotted as a function of time in Figure 11. The plotted data are compared with a model whose parameters for the dust populating the tail’s end point are about midway be-



Figure 10. The Great March Comet of 1843 in the constellation of Cetus seen from Cape Town in the evening of March 4, shortly before it set at 18:36 UT. The comet was nearly 5 days after perihelion and approximately 17° from the Sun in the sky. According to his diary, C. Piazz Smyth went with instruments to the Signal Station on the Lion’s Rump, from where the comet set on the sea horizon (Warner 1980). The painting was made either there or on a nearby beach. Even though the diary does not provide information on the tail length on this day, from the configuration of the bright stars β , η , θ , ζ , and τ Ceti, depicted in the picture, I established that it amounted to $\sim 34^\circ$, including the streamer at the upper end. The tail’s axis extended almost exactly in the antisolar direction, its position angle having equaled 106° . The tail was dominated by plasma, dust may have contributed a little near the head. Note that at its more distant parts the tail was double and that the painting shows the comet’s reflection in water. (Detail of painting; National Maritime Museum, London.)

¹ At the Royal Observatory the comet set on March 4.7753 UT = 18:36.5 UT = 7:50.4 local mean time, 81 minutes after the Sun.

Table 6
Positions of the End of Tail of the Great March Comet of 1843

Time of observation 1843 (UT)	Cometo-centric latitude of Earth	Observation		Model A: $t_{ej} = +0.22$ day, $\beta_{peak} = 0.57$				Model B: $t_{ej} = +0.30$ day, $\beta_{peak} = 0.76$			
		Distance from head	Position angle	Distance from head	Residual $O - C$	Position angle	Residual $O - C$	Distance from head	Residual $O - C$	Position angle	Residual $O - C$
March 8.78	-9.4	33.4	104.7	31.3	+2.1	105.8	-1.1	31.7	+1.7	105.5	-0.8
9.78	-8.6	38.2	103.2	34.6	+3.6	104.8	-1.6	35.0	+3.2	104.5	-1.3
10.77	-7.8	34.0	102.7	37.1	-3.1	104.0	-1.3	37.4	-3.4	103.7	-1.0
13.79	-5.6	44.7	102.4	41.7	+3.0	101.9	+0.5	41.9	+2.8	101.7	+0.7
14.78	-4.9	43.8	102.8	42.5	+1.3	101.4	+1.4	42.6	+1.2	101.3	+1.5
16.78	-3.5	37.0	100.7	43.1	-6.1	100.6	+0.1	43.3	-6.3	100.5	+0.2
17.74	-2.9	46.2	99.7	43.1	+3.1	100.3	-0.6	43.3	+2.9	100.2	-0.5
18.75	-2.2	42.3	102.0	43.1	-0.8	100.0	+2.0	43.2	-0.9	99.9	+2.1
19.75	-1.6	41.9	99.4	42.9	-1.0	99.7	-0.3	43.0	-1.1	99.7	-0.3
22.81	0.0	41.5	99.7	42.1	-0.6	99.3	+0.3	42.0	-0.5	99.3	+0.3

Note.

The observed data for March 17 are from Knorre (1843), for the other dates from Piazz Smyth (Warner 1980).

tween those for the models A and B in Table 6, namely, $t_{ej} = t_{\pi} + 0.25$ day and $\beta_{peak} = 0.65$ the solar gravitational acceleration.

Figure 11 shows that up to about 10 days after perihelion, the substantial contribution from the plasma tail kept the reported lengths above the curve of expected length for the dust tail. This was also true for the tail

lengths measured from Piazz Smyth's paintings in Figures 9 and 10. Beyond about 20 days after perihelion, the reported lengths began to drop below the curve, as the surface brightness of the tail near its end point became too low to detect.

5. COMPARISON OF THE THREE SUNGRAZERS

Notwithstanding, the observed tail length of the Great March Comet of 1843 exceeded the tail lengths of both the Great September Comet of 1882 and Ikeya-Seki, as seen by inspecting Figures 5, 7, and 11. The subject of this section is to investigate why is that so.

Before I directly compare the three sungrazers, I should point out that the already noted Earth's transit of the orbital plane has distinguished the 1843 comet from the other two. The event, which took place four weeks after the comet had passed perihelion, at a time when the tail was still prominent, had two implications for its appearance. One, for several days on either side of the transit time, the tail looked perfectly straight. And two, because of the greater optical depth implied by the edge-on view, the tail appeared a little longer than it otherwise would. The well-known sighting of the 1843 sungrazer over Paris, reproduced in Figure 12, is an excellent example.

Because of the relative orbital positions of the Earth and the Kreutz system's members, a post-perihelion tail displayed by a morning sungrazer in September projects shorter² than an equally long tail of an evening sungrazer in March.³ This was the reason why the reported tail lengths of the 1843 comet exceeded significantly those of the 1882 comet. The striking difference of this kind is plainly apparent from Table 7, in which the observed tails of the three objects are compared at 5, 15, and 25 days after perihelion and which also presents the *maximum* reported tail lengths. Since these were in any case estimates, they were burdened by errors that propagated unevenly into the true tail lengths by conversion from

² This effect has nothing in common with foreshortening associated with the Earth's distance from the orbit plane noted above.

³ One would expect that, because of this effect, more historical Kreutz sungrazers should have been noted in February–March than in September–October, but the results of Hasegawa & Nakano's (2001) investigation do not support this inference.

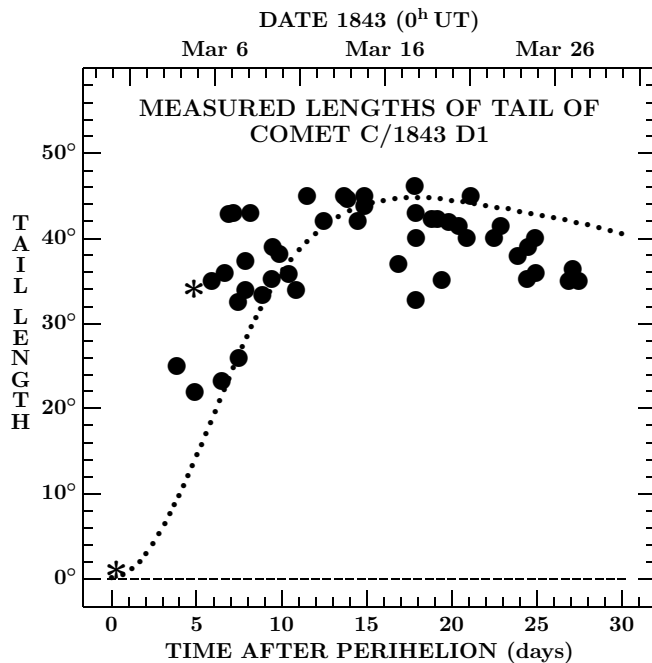


Figure 11. Reported lengths of the post-perihelion tail of the Great March Comet of 1843. The solid circles are the entries from Table C-1, the asterisks are the data obtained from Figures 9 and 10, respectively. The dotted curve shows a dust tail model whose end point contained particles ejected 0.25 day after perihelion and subjected to a radiation pressure acceleration equaling 0.65 the solar gravitational acceleration. Up to about 10 days after perihelion, the contribution from the plasma tail keeps the reported lengths above the curve of expected length for the dust tail. Beyond about 20 days after perihelion, the reported lengths begin to drop below the curve as the surface brightness of the tail near its end point becomes too low to detect.



Figure 12. The Great March Comet of 1843 over Paris in the evening of March 19. The length of the tail was close to 45° , corresponding to 130 million km in space. The Earth was about to cross the orbital plane of the comet (on March 22), which explains that the tail appears nearly perfectly rectilinear. (From Guillemin 1875).

the observed tail lengths. This conversion was accomplished in one of two ways. When the contribution from the plasma tail was obvious, the tail was assumed to extend along the radius vector and its length in space, L , was derived from the observed length, ℓ , with help of the well-known formula,

$$L = \frac{\Delta \sin \ell}{\sin(\phi - \ell)}, \quad (4)$$

where ϕ is the phase angle, Sun–comet head–Earth, and Δ is the comet’s geocentric distance. When the observed tail was believed to be dominated by dust, the length L was derived from the equations for dust-particle dynamics, using the parameters determined in the previous sections.

The tabulated results suggest that the true tail lengths of the 1843 and 1882 sungrazers were comparable, but varied in a wide range, centered approximately on 1 AU. The tail of Ikeya-Seki was shorter than 1 AU. The maximum lengths, reported for Ikeya-Seki by Boethin, appear to be overestimates, especially the higher value, which implied for the true length an unacceptably large value, in excess of 2 AU, regardless of the model used in the conversion. The lower value of 30° was closer to being in line with what one would expect from the other numbers in the table; part of the problem was that a relatively modest difference of 8° in the observed length of the tail changed its true length by fully 1 AU.

The common trait of the tails of the three sungrazers was a major contribution from the plasma component, determining their length in the early post-perihelion times. This rule was unaffected by the sodium tail, detected in comet Ikeya-Seki. As the objects were receding from the Sun, the plasma share was gradually disappearing, until the tails eventually consisted of pure dust.

The sungrazers also displayed similar tail-length variations with time. Shortly after perihelion the tail was growing longer, reached a maximum, and then its length subsided with increasing geocentric distance. Comparison with dust-tail models suggested that in the early post-perihelion period of time the observed tail length exceeded the model prediction, obviously because of the presence of the plasma tail, while months after perihelion the predicted length exceeded the observed length, apparently an effect of the decreasing surface brightness.

The dust tails of the Great March Comet and Ikeya-Seki were also alike in that their end points were populated by the ejecta that left the nucleus a small fraction of a day after perihelion and were subjected to radiation pressure accelerations not exceeding 0.6–0.7 the solar gravitational acceleration. On the other hand, the dust tail of the Great September Comet contained dust particles that appeared to move under radiation pressure accelerations of up to about twice the solar gravitational acceleration and were ejected from the nucleus days after perihelion, possibly an effect of the extensive fragmentation of the nucleus. This sungrazer also displayed a pecu-

Table 7

Tail Lengths of Great March Comet of 1843 (C/1843 D1),
Great September Comet of 1882 (C/1882 R1), and
Ikeya-Seki (C/1965 S1)

	C/1843 D1	C/1882 R1	C/1965 S1
5 days after perihelion:			
Average observed length	34°	15°	15°
Length in space (AU)	0.49	0.55	0.32
15 days after perihelion:			
Average observed length	41°	15°	23°
Length in space (AU)	0.83	0.70	0.60
25 days after perihelion:			
Average observed length	38°	19°	22°
Length in space (AU)	1.45	1.04	0.65
Maximum reported:			
Days after perihelion	18.8	25.6	33.6 (32.6) ^a
Observed length	46°	22°	30° (38°)
Length in space (AU)	1.13	1.35	1.31 (2.30)
Observer	Knorre	Schwab	Boethin

Note.

^a The nominally maximum observed tail length (parenthesized) leads to an unrealistically long tail in space and is deemed erroneous; the second longest observed tail implies a more plausible length in space.

liar feature of a comet in a comet, believed to be a result of near-perihelion disintegration of a companion that had traveled in the same orbit about the Sun for centuries, reaching perihelion nearly 7 days after the main nucleus.

6. CONCLUSIONS

This study was prompted by the important role of the post-perihelion tails in the first sightings of historical appearances of the potential Kreutz sungrazers, implied by the results of Hasegawa & Nakano's (2001) investigation. The objectives are to find out whether it is the plasma or dust component that determines a sungrazer's apparent tail length; variations in the tail length with time and as a function of season; the dynamical properties of the particulate material in the dust tails; peculiar tail features; and the correlation between the observed tail length and true tail length in interplanetary space.

As the pre-perihelion tail completely sublimates at perihelion, the post-perihelion tail development begins from scratch. Under these conditions it is to be expected that shortly after perihelion the tail gradually increases in length, starting from nil. Yet, the rate of this increase often appears to be phenomenally rapid, as illustrated by the Great March Comet of 1843: Less than five days after perihelion its tail length on a painting by Piazzzi Smyth is estimated at 34° (Figure 10). Gigantic dimensions of the plasma tail are made possible by enormous accelerations on CO⁺ and other ionized molecules. The dust tail is at these times much shorter, depending on the peak radiation pressure acceleration that sometimes does not exceed 0.6–0.7 the solar gravitational acceleration. The accelerations in the plasma tail are two or more orders of magnitude higher.

The radiation pressure acceleration is one of two fundamental parameters that govern the motion of a dust particle through the tail. The other is the time of ejection,

while the ejection velocity is also a contributing factor. When the subject of interest is the tail length, the objective is to find the critical parameters of the ejecta at the tail's end point. The tail end of a Kreutz sungrazer weeks after perihelion is usually populated by particles ejected a fraction of the day after perihelion. This is what I find for both Ikeya-Seki and the 1843 sungrazer; the 1882 sungrazer turns out to be a more complicated case. The big help in my effort to solve the problem has been Gill's (1882) photograph and Schmidt's (1882) study of the α' feature seen both visually and on the plate. Even though Schmidt's treatment was tentative, my reanalysis of the motion of the feature — located near the end point of the tail, but far from its sharp edge (populated by the dust subjected to the highest accelerations) — shows that it consisted of grains released later after perihelion than the ejecta at the tail's end point of the two other comets.

Although the data on the tail's end point for the 1882 sungrazer are poor, available information does seem to suggest that the dust tail of this object differed from those of Ikeya-Seki and the 1843 sungrazer, possibly because of the extensive fragmentation of its nucleus near perihelion. The continuing high activity of the nuclear fragments could have made the difference.

The 1882 comet was unique in displaying the bizarre feature of a comet in a comet, brought apparently about by the sudden disintegration of a distant companion nucleus that long followed the main comet in the orbit, passing perihelion nearly 7 days later.

I am unable to confirm a statement often found in popular publications on comets that the true tail length of the Great March Comet of 1843 was 2 AU long, longer than any other comet. Nonetheless, the derived length of nearly 1.5 AU 25 days after perihelion is also respectable. The Earth crossing the comet's orbit plane may have contributed to the reported tail lengths at the time.

An interesting result is a major difference in the degree of foreshortening affecting the post-perihelion tails of the morning sungrazers in September–October and the evening sungrazers in February–March. All other things equal, the evening objects have the projected tails substantially longer than the morning objects.

Addressing finally the initial issue that provoked this investigation, there is no doubt that the discoveries of the historical appearances of potential Kreutz sungrazers, made mostly in the first two weeks after perihelion, as follows from Hasegawa & Nakano's (2001) list, were achieved because of these objects' prominent tails. I also conclude that the tail length was not a critical parameter that facilitated detection; if it were, more potential sungrazers would have been sighted in February–March than in September–October. They were not.

Appendix A

SUMMARY OF
POST-PERHELION TAIL OBSERVATIONS OF
COMET IKEYA-SEKI (C/1965 S1)

This appendix provides lists of the observations of the apparent tail lengths in Table A–1 and of the position angles in Table A–2.

Table A-1
List of Post-Perihelion Tail Length Observations of Comet Ikeya-Seki

Observing time 1965 UT	Tail length ^a	Method ^b	Observing site ^c	Observer & reference
Oct 21.59	1.05	vis	Wrightwood, CA	Capen (Green 1991)
21.72	0.5	vis	Las Cruces, NM	Reese (Green 1991)
21.88	1	vis	Kochi, Japan	Seki (Green 1991)
22.87	1	vis	Kochi, Japan	Seki (Green 1991)
23.12	0.3	vis	Pretoria, South Africa	Bennett (Bennett & Venter 1966)
24.11	>5	vis	Pretoria, South Africa	Venter (Green 1993)
24.11	>5	vis	Pretoria, South Africa	Bennett (Bennett & Venter 1966)
24.13	7	vis	Pretoria, South Africa	Venter (Bennett & Venter 1966)
24.46	1.5	vis	Jacksonville, FL	Simmons (Green 1991)
25.1	9	vis	Pretoria, South Africa	Venter (Green 1993)
25.10	10	vis	Pretoria, South Africa	Bennett (Bennett & Venter 1966)
25.13	8.9	vis*	Pretoria, South Africa	Venter (Bennett & Venter 1966)
25.52	15	vis	Las Cruces, NM	Solberg (Milon 1969, Green 1991)
25.6	12	phot	Mauna Kea, HI	Herring (Milon 1969)
26.10	12.5	vis*	Pretoria, South Africa	Venter (Bennett & Venter 1966)
26.10	13	vis	Pretoria, South Africa	Venter (Green 1993)
26.10	13	vis	Pretoria, South Africa	Bennett (Bennett & Venter 1966)
26.48	9	vis	Chicago, IL	Keen (Green 1985)
26.51	15	vis	Las Cruces, NM	Solberg (Milon 1969)
26.52	15	phot	Las Cruces, NM	Minton (Milon 1969)
26.52	10	vis	Las Cruces, NM	Minton (Green 1991)
26.6	12	phot	Mauna Kea, HI	Herring (Milon 1969)
26.85	25	vis	Kochi, Japan	Seki (Green 1991)
27.12	13.0	vis*	Pretoria, South Africa	Venter (Bennett & Venter 1966)
27.48	16	vis	Chicago, IL	Keen (Green 1985)
27.5	15.3	phot	Tucson, AZ	Larson (Milon 1969)
27.5	17.5	phot	Wrightwood, CA	Capen (Milon 1969)
27.5	17.5	phot	Las Cruces, NM	Minton (Milon 1969)
27.5	17.5	vis	Las Cruces, NM	Solberg (Milon 1969)
27.5	20	vis	Boulder, CO	Johnson (Milon 1969)
27.51	15	phot	Tucson, AZ	Milon (Larson 1966, Milon 1969)
27.51	17	vis	Tucson, AZ	Milon (Larson 1966, Milon 1969)
27.52	15	phot	Tucson, AZ	Larson (1966)
27.6	14	phot	Mauna Kea, HI	Herring (Milon 1969)
27.84	25	vis	Kochi, Japan	Seki (Green 1991)
28.10	19.5	vis*	Pretoria, South Africa	Venter (Bennett & Venter 1966)
28.45	15	vis	Gainesville, FL	Wooten (Milon 1969, Green 1991)
28.48	17	vis	Chicago, IL	Keen (Green 1985)
28.5	15	vis	Las Cruces, NM	Solberg (Milon 1969)
28.51	16.5	phot	Tucson, AZ	Larson (Larson 1966, Milon 1969)
28.6	15	phot	Mauna Kea, HI	Herring (Milon 1969)
28.74	19	vis	Brisbane, Australia	Matchett (Green 1993)
29.10	20	vis	Abastumani, Georgia	Beitrishvili (Green 2001)
29.12	18	phot	Pretoria, South Africa	Bennett (Bennett & Venter 1966)
29.43	19	vis	Mount Vernon, NY	Bortle (Milon 1969, Green 1982)
29.44	17.5	vis	Jacksonville, FL	Simmons (Milon 1969, Green 1991)
29.5	21	vis	Las Cruces, NM	Minton (Milon 1969)
29.5	20	vis	Boulder, CO	Johnson (Milon 1969)
29.5	20	vis	Riverside, CA	Kelsey (Milon 1969)
29.5	17	phot	Las Cruces, NM	Minton (Milon 1969)
29.6	18	phot	Mauna Kea, HI	Herring (Milon 1969)
29.67	15	vis	Nelson, New Zealand	Jones (Green 1987)
29.74	18.8	vis	Brisbane, Australia	Matchett (Green 1993)
30.4	20	vis	Taunton, MA	Delano (Milon 1969)
30.4	18	vis	Charlottesville, VA	Meisel (Milon 1969)
30.4	15	phot	Morgantown, WV	Grady (Milon 1969)
30.43	19	vis	Mount Vernon, NY	Bortle (Milon 1969; Green 1982)
30.43	21	phot	Mount Vernon, NY	Bortle (Milon 1969)
30.43	18	vis	New York, NY	Glenn (Milon 1969, Green 1991)
30.43	20.5	phot	New York, NY	Glenn (Milon 1969)

Table A-1 (continued)

Observing time 1965 UT	Tail length ^a	Method ^b	Observing site ^c	Observer & reference
Oct 30.46	16°	vis	Houston, TX	McCants (Milon 1969, Green 1991)
30.49	16	vis	Las Cruces, NM	Solberg (Milon 1969)
30.5	16	phot	Las Cruces, NM	Minton (Milon 1969)
30.51	20.5	phot	Tucson, AZ	Milon (Larson 1966, Milon 1969)
30.6	19	phot	Mauna Kea, HI	Herring (Milon 1969)
31.09	16	vis	Pretoria, South Africa	Venter (Bennett & Venter 1966, Green 1993)
31.10	19	phot	Pretoria, South Africa	Bennett (Bennett & Venter 1966)
31.17	20	phot	Skalnate Pleso, Slovakia	Antal (1965)
31.4	22	phot	New York, NY	Pearson (Milon 1969)
31.4	18	phot	Morgantown, WV	Grady (Milon 1969)
31.43	20	vis	Mount Vernon, NY	Bortle (Milon 1969, Green 1982)
31.43	15	vis	New York, NY	Glenn (Milon 1969, Green 1991)
31.43	20	vis	Charlottesville, VA	Meisel (Milon 1969)
31.47	19	vis	Chicago, IL	Keen (Green 1985)
31.50	20	vis	Las Cruces, NM	Solberg (Milon 1969)
31.6	22	phot	Mauna Kea, HI	Herring (Milon 1969)
31.67	17	vis	Nelson, New Zealand	Jones (Green 1987)
Nov 1.10	20	vis	Pretoria, South Africa	Bennett (Bennett & Venter 1966)
1.4	23	vis	Vinton, VA	Smith (Milon 1969)
1.41	20	vis	Taunton, MA	Delano (Green 1991)
1.42	18	vis	Mount Vernon, NY	Bortle (Milon 1969, Green 1982)
1.43	20	vis	Charlottesville, VA	Meisel (Milon 1969)
1.47	23	vis	Chicago, IL	Keen (Green 1985)
1.50	21	vis	Las Cruces, NM	Solberg (Milon 1969)
1.5	20	vis	Boulder, CO	Johnson (Milon 1969)
1.84	20	vis	Kochi, Japan	Seki (Milon 1969, Green 1991)
2.10	18	vis	Pretoria, South Africa	Venter (Bennett & Venter 1966)
2.10	19.8	vis*	Pretoria, South Africa	Venter (Bennett & Venter 1966)
2.17	18	phot	Skalnate Pleso, Slovakia	Antal (1965)
2.39	15	vis	New York, NY	Glenn (Green 1991)
2.4	17.5	vis	Vinton, VA	Smith (Milon 1969)
2.41	20	vis	Taunton, MA	Delano (Milon 1969, Green 1991)
2.42	21	vis	Mount Vernon, NY	Bortle (1969), Green (1982)
2.44	18.5	vis	Jacksonville, FL	Simmons (Milon 1969, Green 1991)
2.44	22	vis	Elizabeth, WV	Conger (Milon 1969, Green 1991)
2.47	25	vis	Chicago, IL	Keen (Green 1985)
2.5	25	vis	Dallas, TX	Swann (Milon 1969)
2.5	26	phot	Tucson, AZ	Larson (1966)
2.51	22	vis	Las Cruces, NM	Solberg (Milon 1969)
2.52	19.5	phot	Tucson, AZ	Milon (1969)
2.6	24	phot	Mauna Kea, HI	Herring (Milon 1969)
2.66	21	vis	Nelson, New Zealand	Jones (Green 1987)
2.85	24	vis	Abra, Philippines	Boethin (Milon 1969, Green 1991)
3.43	21.3	vis	Jacksonville, FL	Simmons (Milon 1969, Green 1991)
3.43	24	vis	Elizabeth, WV	Conger (Milon 1969, Green 1991)
3.5	22	vis	Boulder, CO	Johnson (Milon 1969)
3.5	22	vis	Las Cruces, NM	Solberg (Milon 1969)
3.6	25	phot	Mauna Kea, HI	Herring (Milon 1969)
3.83	15	vis	Kochi, Japan	Seki (Green 1991)
3.85	30	vis	Abra, Philippines	Boethin (Green 1991)
4.06	>13	vis	Kazan, Russia	Kadomskiy (Green 2001)
4.43	23	vis	Jacksonville, FL	Simmons (Milon 1969, Green 1991)
4.47	26	vis	Chicago, IL	Keen (Green 1985)
4.50	22	vis	Las Cruces, NM	Solberg (Milon 1969)
4.5	22.5	vis	Las Cruces, NM	Haas (Milon 1969)
4.85	25	vis	Abra, Philippines	Boethin (Green 1991)
5.10	20	vis	Pretoria, South Africa	Venter (Bennett & Venter 1966, Green 1993)
5.12	23	vis	Pretoria, South Africa	Bennett (Bennett & Venter 1966)
5.13	25	vis	Nauchnyy, Crimea	Chernykh (Green 2001)
5.42	20	vis	Mount Vernon, NY	Bortle (Milon 1969, Green 1982)

Table A-1 (continued)

Observing time 1965/66 UT	Tail length ^a	Method ^b	Observing site ^c	Observer & reference
Nov 5.42	22°	vis	Taunton, MA	Delano (Milon 1969, Green 1991)
5.50	25*	vis	Las Cruces, NM	Solberg (Milon 1969, Green 1991)
6.40	23.8*	vis	New York, NY	Glenn (Milon 1969, Green 1991)
6.42	25	vis	Mount Vernon, NY	Bortle (Milon 1969, Green 1982)
6.50	23*	vis	Las Cruces, NM	Solberg (Milon 1969, Green 1991)
7.07	23	vis	Pretoria, South Africa	Bennett (Bennett & Venter 1966)
7.50	22	vis	Las Cruces, NM	Solberg (Milon 1969)
7.5	25	vis	Las Cruces, NM	Haas (Milon 1969)
8.08	20.7	vis*	Pretoria, South Africa	Venter (Bennett & Venter 1966)
8.09	22	vis	Pretoria, South Africa	Venter (Green 1993)
9.86	>5	vis	Kochi, Japan	Seki (Green 1991)
14.46	1	vis	Chicago, IL	Keen (Green 1985)
15.43	2.5	vis	Mount Vernon, NY	Bortle (Green 1982)
17.05	24	vis	Pretoria, South Africa	Venter (Bennett & Venter 1966)
17.08	>5	vis	Pretoria, South Africa	Bennett (Bennett & Venter 1966)
17.81	>5	vis	Kochi, Japan	Seki (Green 1991)
18.61	5	vis	Nelson, New Zealand	Jones (Green 1987)
19.09	22	vis	Pretoria, South Africa	Venter (Green 1993)
19.09	22	vis	Pretoria, South Africa	Bennett (Bennett & Venter 1966)
20.44	12	vis	Elizabeth, WV	Conger (Green 1991)
20.51	19*	vis	Las Cruces, NM	Solberg (Milon 1969, Green 1991)
20.61	3.5	vis	Nelson, New Zealand	Jones (Green 1987)
21.85	23	vis	Abra, Philippines	Boethin (Milon, 1969, Green 1991)
22.61	1.0	vis	Nelson, New Zealand	Jones (Green 1987)
22.81	38	vis	Abra, Philippines	Boethin (Green 1991)
23.77	30	vis	Abra, Philippines	Boethin (Milon 1969, Green 1991)
24.06	17.4	vis*	Pretoria, South Africa	Venter (Bennett & Venter 1966)
24.09	20	vis	Pretoria, South Africa	Bennett (Bennett & Venter 1966)
24.69	30	vis	Abra, Philippines	Boethin (Green 1991)
25.04	12.9	vis*	Pretoria, South Africa	Venter (Bennett & Venter 1966)
26.59	1.3	vis	Nelson, New Zealand	Jones (Green 1987)
29.43	0.7	vis	Mount Vernon, NY	Bortle (Green 1982)
29.5	29	phot	Tucson, AZ	Milon (Larson 1066, Milon 1969)
29.5	10	vis	Tucson, AZ	Milon (Larson 1966)
29.62	6	vis	Nelson, New Zealand	Jones (Green 1987)
30.62	4	vis	Nelson, New Zealand	Jones (Green 1987)
Dec 1.08	>12	vis	Pretoria, South Africa	Bennett (Bennett & Venter 1966)
1.61	3.5	vis	Nelson, New Zealand	Jones (Green 1987)
3.79	5	vis	Abra, Philippines	Boethin (Green 1991)
4.5	25	phot	Tucson, AZ	Milon (Larson 1966, Milon 1969)
4.5	7	vis	Tucson, AZ	Milon (Larson 1966)
5.63	0.8	vis	Nelson, New Zealand	Jones (Green 1987)
17.60	0.5	vis	Nelson, New Zealand	Jones (Green 1987)
31.38	1.5	phot	Mount Palomar, CA	Tammann (1966)
Jan 14.29	1.3	phot	Mount Palomar, CA	Tammann (1966)

Notes.

^a Tail lengths marked with an asterisk is an average of the different values listed in the two references.

^b Tail lengths marked in this column with vis* were derived by the author from Venter's estimates of the equatorial coordinates of the tail's tip.

^c In some cases the observing site has been difficult to establish; in others the actual location may be on the outskirts or in the proximity of the listed city.

Table A-2

List of Position Angle Observations of Post-Perihelion Tail of Comet Ikeya-Seki

Observing time 1965 UT	Position angle ^a	Method ^b	Observer & reference
Oct 24.11	315°	vis	Bennett (Bennett & Venter 1966)
24.46	305*	vis	Simmons (Green 1991)
25.13	278	vis	Venter (Bennett & Venter 1966)
25.64	278	phot	Herring (Milon 1969)
26.10	280	vis	Venter (Green 1993)
26.10	283	vis*	Venter (Bennett & Venter 1966)
26.10	280	vis	Bennett (Bennett & Venter 1966)
26.52	265	vis	Minton (Green 1993)
27.12	272	vis*	Venter (Bennett & Venter 1966)
27.51	274	phot	Milon (1969)
28.10	254	vis*	Venter (Bennett & Venter 1966)
28.51	273	phot	B. Smith (Milon 1969)
28.74	274	vis	Matchett (Green 1993)
29.12	263	phot	Bennett (Bennett & Venter 1966)
29.43	267	vis	Bortle (Green 1982)
29.44	270*	vis	Simmons (Green 1991)
29.50	272	phot	B. Smith (Milon 1969)
29.67	270	vis	Jones (Green 1987)
29.74	270	vis	Matchett (Green 1993)
30.43	268	vis	Bortle (Green 1982)
30.46	275	vis	McCants (Green 1991)
30.51	271	phot	Milon (1969)
31.10	283	photo	Bennett (Bennett & Venter 1966)
31.43	266	vis	Bortle (Green 1982)
31.49	269	phot	B. Smith (Milon 1969)
Nov 1.42	270	vis	Bortle (Green 1982)
1.49	270	phot	B. Smith (Milon 1969)
2.10	282	vis*	Venter (Bennett & Venter 1966)
2.42	280	vis	Bortle (Green 1982)
2.44	271*	vis	Simmons (Green 1991)
2.44	262*	vis	Conger (Green 1991)
2.52	268	phot	Milon (1969)
2.66	278	vis	Jones (1987)
2.85	274*	vis	Boethin (1991)
3.54	269	phot	Capen (Milon 1969)
3.85	249*	vis	Boethin (1991)
4.43	265*	vis	Simmons (1991)
4.52	268	photo	Capen (Milon 1969)
5.12	280	vis	Bennett (Bennett & Venter 1966)
5.42	275	vis	Bortle (Green 1982)
5.50	269	phot	B. Smith (Milon 1969)
6.42	276	vis	Bortle (Green 1982)
6.52	268	photo	Capen (Milon 1969)
8.08	272	vis*	Venter (Bennett & Venter 1966)
15.43	271	vis	Bortle (Green 1982)
17.05	290	vis	Venter (Bennett & Venter 1966)
17.08	279	vis	Bennett (Bennett & Venter 1966)
18.61	285	vis	Jones (Green 1987)
20.44	265*	vis	Conger (Green 1991)
20.61	288	vis	Jones (Green 1987)
21.85	288*	vis	Boethin (Green 1991)
22.61	290	vis	Jones (Green 1987)
22.81	297*	vis	Boethin (Green 1991)
23.77	302*	vis	Boethin (Green 1991)
24.06	292	vis*	Venter (Bennett & Venter 1966)
24.69	302*	vis	Boethin (Green 1991)
25.04	295	vis*	Venter (Bennett & Venter 1966)
26.59	300	vis	Jones (Green 1987)
29.43	290	vis	Bortle (Green 1982)

Table A-2 (continued)

Observing time 1965 UT	Position angle ^a	Method ^b	Observer & reference
Nov 30.62	294°	vis	Jones (Green 1987)
Dec 1.61	300	vis	Jones (Green 1987)
5.63	295	vis	Jones (Green 1987)
17.60	325	vis	Jones (Green 1987)

Notes.

^a When marked with an asterisk, the reported position angle has been corrected by adding 180°.

^b Asterisk in this column indicates that the position angle was derived by the author from Venter's equatorial coordinates of the tail's tip.

Appendix B

SUMMARY OF POST-PERHELION TAIL OBSERVATIONS OF GREAT SEPTEMBER COMET OF 1882 (C/1882 R1)

This appendix provides a list of the apparent tail length observations in Table B-1.



Table B-1
List of Post-Perihelion Tail Length Observations of Comet C/1882 R1

Observing time 1882 UT	Tail length	Observing site	Observer & reference
Sept 23.46	15°	Nashville	Barnard (1883, 1884)
23.85	15	Melbourne Obs.	Ellery (1882a, 1882b)
24.46	15	Nashville	Barnard (1883, 1884)
25.28	15	at sea (Carribean)	Schwab (1883)
28.29	14	at sea	Schwab (1883)
29.17	20	Vienna	Palisa (1882)
29.4	15	U.S. Naval Obs.	Skinner (Winlock 1884)
30.27	12	at sea	Schwab (1883)
30.4	15	U.S. Naval Obs.	Frisby (Winlock 1884)
Oct 2.24	12	at sea	Schwab (1883)
3.29	14	at sea	Schwab (1883)
3.5	19	U.S. Naval Obs.	Winlock (1884)
4.42	15	L. McCormick Obs.	Jones (Leavenworth & Jones 1915)
5.26	15.2	at sea	Schwab (1883)
5.4	17-18	U.S. Naval Obs.	Frisby (Winlock 1884)
5.42	15	L. McCormick Obs.	Jones (Leavenworth & Jones 1915)
6.19	20	Dresden	von Engelhardt (1882, 1883)
6.32	16.5	at sea	Schwab (1883)
6.41	15-16	L. McCormick Obs.	Jones (Leavenworth & Jones 1915)
7.16	15	Breslau	Galle (1882)
7.19	20	Dresden	von Engelhardt (1882, 1883)
7.4	17	U.S. Naval Obs.	Winlock (1884)
7.41	16	L. McCormick Obs.	Jones (Leavenworth & Jones 1915)
8.18	18	Dresden	von Engelhardt (1882, 1883)
8.4	17	U.S. Naval Obs.	Winlock (1884)
9.39	18	L. McCormick Obs.	Jones (Leavenworth & Jones 1915)
10.35	18.7	at sea	Schwab (1883)
10.4	14	U.S. Naval Obs.	Winlock (1884)
11.4	16	U.S. Naval Obs.	Winlock (1884)
13.2	17	Lyon	André (1882)
13.37	22	at sea	Schwab (1883)
15.39	18	L. McCormick Obs.	Jones (Leavenworth & Jones 1915)
15.4	17	U.S. Naval Obs.	Winlock (1884)
16.33	21	at sea	Schwab (1883)
16.44	17-18	Nashville	Barnard (1883, 1884)
20.44	17-18	Nashville	Barnard (1883, 1884)
23.2	15	Barham, England	Ledger (1882)
23.39	20	L. McCormick Obs.	Jones (Leavenworth & Jones 1915)
24.39	20	L. McCormick Obs.	Jones (Leavenworth & Jones 1915)
25.4	12	U.S. Naval Obs.	Winlock (1884)
27.44	17.8	Nashville	Barnard (1883, 1884)
29.19	10-12	Dresden	von Engelhardt (1882, 1883)
Nov 1.44	18.8	Nashville	Barnard (1883, 1884)
3.4	10-12	U.S. Naval Obs.	Winlock (1884)
5.41	20	L. McCormick Obs.	Jones (Leavenworth & Jones 1915)
7.39	18.1	Nashville	Barnard (1883, 1884)
9.4	10	U.S. Naval Obs.	Winlock (1884)
11.39	17.7	Nashville	Barnard (1883, 1884)
12.41	20	L. McCormick Obs.	Jones (Leavenworth & Jones 1915)
13.2	>21	Punta Arenas	Schwab (1883)
14.4	10	U.S. Naval Obs.	Winlock (1884)
16.39	17.2	Nashville	Barnard (1883, 1884)
16.4	10	U.S. Naval Obs.	Winlock (1884)
17.30	21	at sea	Schwab (1883)
19.4	10	U.S. Naval Obs.	Winlock (1884)
21.4	15	U.S. Naval Obs.	Winlock (1884)
22.4	11	U.S. Naval Obs.	Winlock (1884)
23.4	12	U.S. Naval Obs.	Winlock (1884)
Dec 3.4	6-7	U.S. Naval Obs.	Winlock (1884)
8.3	8	U.S. Naval Obs.	Winlock (1884)

Table B-1 (continued)

Observing time 1882 UT	Tail length	Observing site	Observer & reference
Dec 12.3	8	U.S. Naval Obs.	Winlock (1884)
Jan 2.86	12	Athens Obs.	Schmidt (1883)
3.85	11	Athens Obs.	Schmidt (1883)
10.83	8	Athens Obs.	Schmidt (1883)
28.81	5.5	Athens Obs.	Schmidt (1883)
30.82	3	Athens Obs.	Schmidt (1883)
30.88	8	at sea	Schwab (1883)
31.85	>3	Athens Obs.	Schmidt (1883)
31.95	7.5	at sea	Schwab (1883)
Feb 2.8	5.5	Sunderland, England	Backhouse (1883)
5.75	2	Athens Obs.	Schmidt (1883)
7.84	4.5	at sea	Schwab (1883)
12.0	6	Córdoba Obs.	Gould (1883)

Appendix C

SUMMARY OF POST-PERHELION TAIL OBSERVATIONS OF GREAT MARCH COMET OF 1843 (C/1843 D1)

This appendix provides a list of the apparent tail length observations in Table C-1.



Table C-1
List of Post-Perihelion Tail Length Observations of Comet C/1843 D1

Observing time 1843 UT	Tail length	Observing site	Observer & reference
March	3.77	25°	Cape Obs. Piazz Smyth (Warner 1980)
	4.8	22	Cape Colony Maclean (1844)
	5.8	35	Cape Obs. Piazz Smyth (Warner 1980)
	6.4	23.3	Tasmania Kay (1843)
	6.58	36	Trevandrum Obs. Caldecott (1846)
	6.8	42.9	Island of St. Helena Brand (1844)
	7.07	43.0	South Pacific Tucker (1843)
	7.35	32.5	Auckland Haile (1843)
	7.4	26	Tasmania Kay (1843)
	7.8	>34	Cape Colony Maclean (1844)
	7.8	37.4	Island of St. Helena Brand (1844)
	8.07	43	South Pacific Tucker (1843)
	8.78	33.4	Cape Obs. Piazz Smyth (Warner 1980)
	9.33	35.2	Auckland Haile (1843)
	9.4	39	Tasmania Kay (1843)
	9.78	38.2	Cape Obs. Piazz Smyth (Warner 1980)
	10.34	35.8	Auckland Haile (1843)
	10.77	34.0	Cape Obs. Piazz Smyth (Warner 1980)
	11.4	45	Tasmania Kay (1843)
	12.4	42	Tasmania Kay (1843)
	13.58	45	Trevandrum Obs. Caldecott (1846)
	13.79	44.7	Cape Obs. Piazz Smyth (Warner 1980)
	14.4	42	Tasmania Kay (1843)
	14.78	43.8	Cape Obs. Piazz Smyth (Warner 1980)
	14.78	45	Nice Cooper (1843)
	16.78	37.0	Cape Obs. Piazz Smyth (Warner 1980)
	17.74	46.2	Nikolayev Knorre (1843)
	17.8	43	Cape Colony Maclean (1844)
	17.8	32.8	Island of St. Helena Brand (1844)
	17.81	40	Greenwich Dunkin (Airy 1845)
	18.75	42.3	Cape Obs. Piazz Smyth (Warner 1980)
	18.78	40	Vienna von Littrow (1843)
	19.07	42.3	South Pacific Tucker (1843)
	19.33	41.8	Auckland Haile (1843)
	19.75	41.9	Cape Obs. Piazz Smyth (Warner 1980)
	20.33	41.5	Auckland Haile (1843)
	20.80	40	Berlin Galle (Schumacher 1843)
	21.05	45.0	South Pacific Tucker (1843)
	22.4	40	Tasmania Kay (1843)
	22.81	41.5	Cape Obs. Piazz Smyth (Warner 1980)
	23.8	38	Cape Colony Maclean (1844)
	24.35	35.2	Auckland Haile (1843)
	24.4	39	Tasmania Kay (1843)
	24.82	40	Greenwich Glaisher (Airy 1845)
	24.86	36	Greenwich Dunkin (Airy 1843)
	26.8	35	Cape Colony Maclean (1844)
	27.03	36.4	South Pacific Tucker (1843)
	27.4	35	Tasmania Kay (1843)

REFERENCES

- Airy, G. B. 1845, *Greenwich Astron. Magnet. Met. Roy. Obs.* (Series 2), 5, C103
- André, Ch. 1882, *Astron. Nachr.*, 103, 349
- Antal, M. 1965, *IAU Circ.* 1944
- Backhouse, T. W. 1883, *Nature*, 27, 338
- Barnard, E. E. 1883, *Astron. Nachr.*, 104, 267
- Barnard, E. E. 1884, *Sid. Mess.*, 3, 168
- Bennett, J. C., & Venter, S. C. 1966, *Mon. Not. Astron. Soc. South Africa*, 25, 12
- Brand, G. 1844, *Mon. Not. Roy. Astron. Soc.*, 6, 136
- Caldecott, J. 1846, *Mem. Roy. Astron. Soc.*, 15, 229
- Cooper, E. 1843, *Astron. Nachr.*, 20, 291
- Ellery, R. J. L. 1882a, *Observ.*, 5, 368
- Ellery, R. J. L. 1882b, *Astron. Nachr.*, 103, 349
- Engelhardt, B. von 1882, *Astron. Nachr.*, 103, 327
- Engelhardt, B. von 1883, *Astron. Nachr.*, 105, 267
- Galle, J. G. 1882, *Astron. Nachr.*, 103, 319
- Gill, D. 1882, *Mon. Not. Roy. Astron. Soc.*, 43, 53
- Gill, D. 1911, *Ann. Cape Obs.*, 2, 3
- Gould, B. A. 1883, *Astron. Nachr.*, 105, 185
- Green, D. W. E. 1982, *Int. Comet Quart.*, 4, 81
- Green, D. W. E. 1985, *Int. Comet Quart.*, 7, 53
- Green, D. W. E. 1987, *Int. Comet Quart.*, 9, 104
- Green, D. W. E. 1991, *Int. Comet Quart.*, 13, 9
- Green, D. W. E. 1993, *Int. Comet Quart.*, 15, 115
- Green, D. W. E. 2001, *Int. Comet Quart.*, 23, 110
- Guillemin, A. 1875, *Les Comètes*. Paris: Hachette. (English translation and edition: Glaisher, J. 1877, *The World of Comets*. London: Sampson Low, Martson, Searle & Rivington)
- Gustafson, B. A. S. 1985, in *Properties and Interactions of Interplanetary Dust*, Proc. IAU Coll. 85, ed. R. H. Giese & P. Lamy. Dordrecht, Netherlands: D. Reidel Publ. Co., 227
- Hagughney, L. C., Bader, M., & Innes, R. 1967, *AJ*, 72, 1166
- Haile, J. C. 1843, *Mon. Not. Roy. Astron. Soc.*, 6, 5
- Hasegawa, I., & Nakano, S. 2001, *Publ. Astron. Soc. Japan*, 53, 931
- Herring, A. K. 1966, *Comm. Lunar Plan. Lab.*, 4, 141
- Kapoor, R. C. 2021, *J. Astron. Hist. Herit.*, 24, 703
- Kay, J. H. 1843, *Mon. Not. Roy. Astron. Soc.*, 6, 5
- Knorre, K. 1843, *Astron. Nachr.*, 20, 345
- Kortazzi, J. 1882, *Astron. Nachr.*, 104, 61
- Krishan, V., & Sivaraman, K. R. 1982, *Moon Plan.*, 26, 209
- Krishna Swamy, K. S. 1978, *Astrophys. Space Sci.*, 57, 491
- Larson, S. M. 1966, *Comm. Lunar Planet. Lab.*, 4, 145
- Leavenworth, F. P., & Jones, J. 1915, *Publ. Leander McCormick Obs.*, 1, 9
- Ledger, E. 1882, *Observ.*, 5, 328
- Littrow, C. L. von 1843, *Astron. Nachr.*, 20, 291
- Macleay, G. 1844, *Mon. Not. Roy. Astron. Soc.*, 6, 76
- Marsden, B. G. 1967, *AJ*, 72, 1170
- Matyagin, V. S., Sabitov, S. N., & Kharitonov, A. V. 1968, *Sov. Astron.*, 11, 863
- Milon, D. 1969, *Stroll. Astron.*, 21, 146
- Palisa, J. 1882, *Astron. Nachr.*, 103, 175
- Piazzi Smyth, C. 1846, *Mon. Not. Roy. Astron. Soc.*, 7, 42
- Riccò, A. 1882, *Astron. Nachr.*, 103, 281
- Roemer, E. 1966, *Publ. Astron. Soc. Pacific*, 78, 83
- Saito, K., Isobe, S., Nishioka, K., & Ishii, T. 1981, *Icarus*, 47, 351
- Schmidt, J. F. J. 1882, *Astron. Nachr.*, 104, 89
- Schmidt, J. F. J. 1883, *Astron. Nachr.*, 104, 361
- Schumacher, H. C. 1843, *Astron. Nachr.*, 20, 289
- Schwab, F. 1883, *Astron. Nachr.*, 105, 3
- Sekanina, Z. 1982, in *Comets*, ed. L. L. Wilkening. Tucson: University of Arizona, 251
- Sekanina, Z. 1984, *Icarus*, 58, 81
- Sekanina, Z. 2000, *ApJ*, 545, L69
- Sekanina, Z. 2002, *ApJ*, 566, 577
- Sekanina, Z. 2021, eprint arXiv:2109.01297
- Sekanina, Z. 2022, eprint arXiv:2202.01164
- Sekanina, Z., & Chodas, P. W. 2012, *ApJ*, 757, 127 (33 pp)
- Sekanina, Z., & Kracht, R. 2022, eprint arXiv:2206.10827
- Tammann, G. A. 1966, *IAU Circ.* 1952
- Thompson, W. T. 2009, *Icarus*, 200, 351
- Thompson, W. T. 2015, *Icarus*, 261, 122
- Tucker, J. J. 1843, *Mon. Not. Roy. Astron. Soc.*, 6, 3
- Warner, B. 1980, *Mon. Not. Roy. Astron. Soc. South Africa*, 39, 69
- Weinberg, J. L., & Beeson, D. E. 1976a, in *The Study of Comets*, NASA SP-393, ed. B. Donn, M. Mumma, W. Jackson, M. A'Hearn, & R. Harrington. Washington, DC: U.S. GPO, 92
- Weinberg, J. L., & Beeson, D. E. 1976b, *A&A*, 48, 151
- Winlock, W. C. 1884, *Astron. Met. Obs. U.S. Naval Obs.*, 20A, 1